

Manuscript Details

Manuscript number	JASREP_2017_16
Title	Iron and Copper Production at Iron Age Ashkelon: Implications for the Organization of Levantine Metal Production
Short title	Iron and Copper Production at Ashkelon
Article type	Research Paper

Abstract

Understanding the spatial distribution of different craft production activities is an essential part of any investigation into the organization of production. In the Iron Age southern Levant, discussions of the rise of iron often revolve around the relative organization of bronze and iron production. For these reasons, identifying where different stages of metal production occurred is essential for testing models of technological change during this period. This study reviews the challenges of identifying different stages of metal production from often-ephemeral residues found at settlement sites, with particular emphasis on the question of urban iron smelting in the early Iron Age southern Levant. These considerations are applied to the analysis of a small but significant assemblage of metal production remains from Iron IIB Ashkelon (c. 8th century BC), using macroscopic observations, chemical analysis, and microscopy. The results of these analyses support the conclusion that multiple iron production processes—likely including both smelting and smithing—took place in or near a domestic quarter at Ashkelon. With one or two exceptions, copper production residues are restricted to secondary refining and casting residues. Copper smelting was carried out elsewhere. If this pattern holds as more urban production debris is recognized and analyzed, such differences in the relative organization of iron and copper-alloy production may provide clues as to why iron production expanded dramatically in the early 1st millennium BC.

Keywords	Metallurgy; Craft Production; Levant; Smelting; Smithing; Slag; Crucible
Corresponding Author	Nathaniel L. Erb-Satullo
Corresponding Author's Institution	Harvard University
Order of Authors	Nathaniel L. Erb-Satullo, Joshua T. Walton
Suggested reviewers	Adi Eliyahu-Behar, Erez Ben-Yosef, Shadreck Chirikure, Jane Humphris, Aaron Shugar

Submission Files Included in this PDF

File Name [File Type]

CuFeProdAshkelon_Revisions_CoverLetter.doc [Cover Letter]

Response to Reviewers_final.docx [Response to Reviewers]

CuFeProdAshkelon_Highlights.docx [Highlights]

Ashkelon_GraphicalAbstract.tif [Graphical Abstract]

CuFeProdAshkelon_revisions_final_plaintext.docx [Manuscript File]

Fig1_MapOfSites.tif [Figure]

Fig1_MapOfSites_gs.tif [Figure]

Fig2_Plan_revised2.tif [Figure]

Fig3_MacroPhotos_rev.tif [Figure]

Fig3_MacroPhotos_rev_gs.tif [Figure]

Fig4_SmithingSlags.tif [Figure]

Fig4_SmithingSlags_gs.tif [Figure]

Fig5_IronOxidesIronMetal_rev.tif [Figure]

Fig5_IronOxidesIronMetal_rev_gs.tif [Figure]

Fig6_TapSlags.tif [Figure]

Fig6_TapSlags_gs.tif [Figure]

Fig7_FusedOre.tif [Figure]

Fig8_A14.tif [Figure]

Fig8_A14_gs.tif [Figure]

Fig9_CuSlags.tif [Figure]

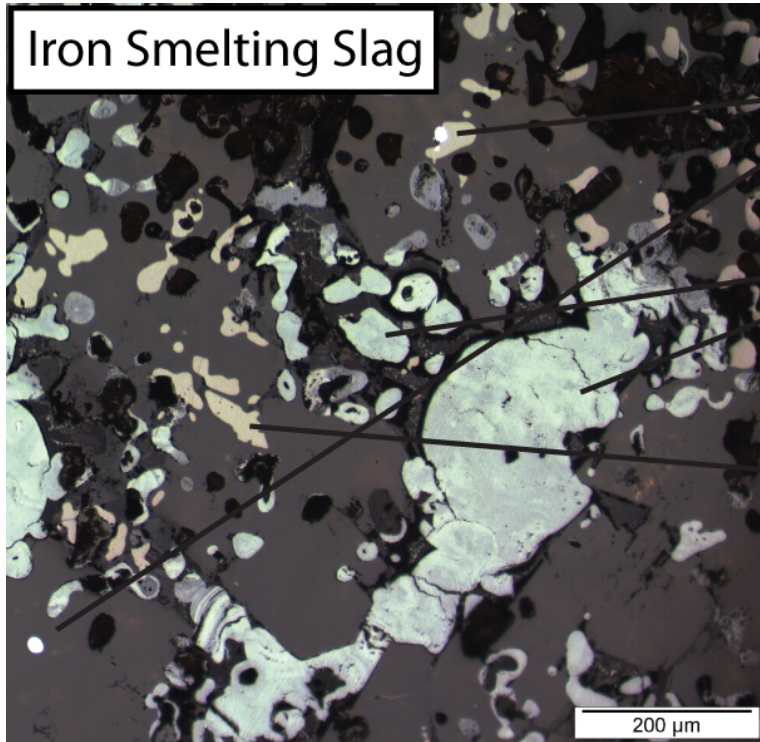
Fig10_A21.tif [Figure]

Fig10_A21_gs.tif [Figure]

To view all the submission files, including those not included in the PDF, click on the manuscript title on your EVISE Homepage, then click 'Download zip file'.

- We review the challenges facing the identification of metal production stages.
- Iron and copper-alloy production debris from Iron Age Ashkelon were analyzed.
- Mineralogical and morphological data point to multiple stages of iron production.
- Copper refining took place at the site, but probably not smelting.
- Comparing spatial patterns of metal production may help explain the spread of iron.

Iron Smelting Slag



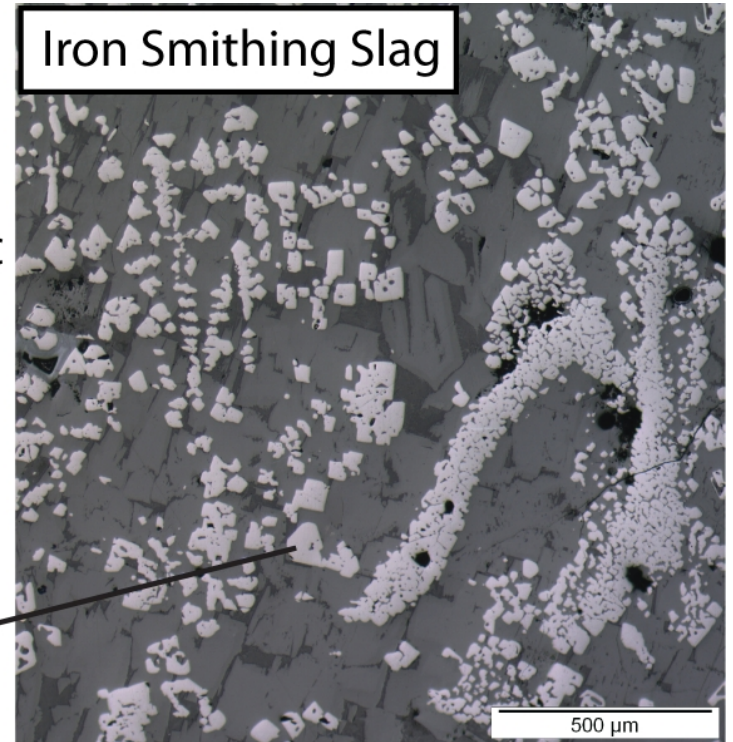
Metallic Iron

Corroded Metallic
Iron

Wüstite (FeO)

Magnetite (Fe₃O₄)

Iron Smithing Slag



500 μm

IRON AND COPPER PRODUCTION AT IRON AGE ASHKELON: IMPLICATIONS FOR THE ORGANIZATION
OF LEVANTINE METAL PRODUCTION

Nathaniel L. Erb-Satullo¹

Joshua T. Walton²

¹Department of Anthropology, Harvard University, 11 Divinity Ave, Cambridge, MA, 02138
USA; nsatullo@fas.harvard.edu; Phone: +1-413-441-2331; Corresponding Author

²History Department, Capital University, 1 College Ave, Columbus, OH, 43209 USA;
jtwalton@gmail.com

Abstract

Understanding the spatial distribution of different craft production activities is an essential part of any investigation into the organization of production. In the Iron Age southern Levant, discussions of the rise of iron often revolve around the relative organization of bronze and iron production. For these reasons, identifying where different stages of metal production occurred is essential for testing models of technological change during this period.

This study reviews the challenges of identifying different stages of metal production from often-ephemeral residues found at settlement sites, with particular emphasis on the question of urban iron smelting in the early Iron Age southern Levant. These considerations are applied to the analysis of a small but significant assemblage of metal production remains from Iron IIB

Ashkelon (c. 8th century BC), using macroscopic observations, chemical analysis, and microscopy.

The results of these analyses support the conclusion that multiple iron production processes--likely including both smelting and smithing—took place in or near a domestic quarter at Ashkelon. With one or two exceptions, copper production residues are restricted to secondary refining and casting residues. Copper smelting was carried out elsewhere. If this pattern holds as more urban production debris is recognized and analyzed, such differences in the relative organization of iron and copper-alloy production may provide clues as to why iron production expanded dramatically in the early 1st millennium BC.

Keywords

Metallurgy; Craft Production; Levant; Smelting; Smithing; Slag; Crucible

1. Introduction

Recent research has expanded the number of sites with well-studied iron production remains in the southern Levant (**Fig. 1**) (Eliyahu-Behar, et al., 2008; Eliyahu-Behar, et al., 2012; Eliyahu-Behar, et al., 2013; Veldhuijzen and Rehren, 2007; Veldhuijzen, 2009; Yahalom-Mack, et al., 2014a; Yahalom-Mack and Eliyahu-Behar, 2015). These studies have dramatically increased our understanding of iron production between 1200 and 600 BC, during which time iron went from a valued rarity to a ubiquitous material. The spatial organization of the *chaîne opératoire* has been a significant concern in this research. Reconstructing where different stages of production took place is crucial for understanding the role of iron in society, particularly in comparison with that of bronze.

An emerging consensus links the spread of iron in the southern Levant with a desire to control (or to maintain more direct access to) supplies of metal (Veldhuijzen, 2012; Yahalom-Mack and Eliyahu-Behar, 2015). Nevertheless, the precise nature of that control, and what social level it operated at, remains very unclear. This consensus is in some ways a reformulation of older claims, now largely abandoned, about a shortage of copper and/or tin driving the spread of iron-making technologies (for evolving views on this issue, see Maddin, et al., 1977:23; McNutt, 1990:153-154; Mirau, 1997:104-105; Muhly, 1992:17; Snodgrass, 1971:237-238). More recent perspectives on the spread of iron stress the appeal of a new locally-available metal within an increasingly decentralized political system as the driving factor (Mirau, 1997:110-111). While trade networks were undoubtedly transformed after the Late Bronze Age collapse, new copper industries emerged to supply the Southern Levant. The Iron Age saw a dramatic expansion in copper production in the Wadi Arabah (Ben-Yosef, et al., 2010:743; Ben-Yosef, et al., 2012;

Levy, et al., 2004; Levy, et al., 2008; Yahalom-Mack, et al., 2014b), so economic forces contributing to the adoption of iron were probably more complex than an acute region-wide shortage of bronze. The proper identification of production residues is vital to reconstructing the economic system of the southern Levant, and the role that iron production played in the emergence and maintenance of new Iron Age political formations.

Recent research on iron production in the southern Levant has revealed several important technological and organizational features. First, some segments of bronze and iron production sequences were carried out in the same workshops, suggesting that the same craftspeople may have worked both metals. At Iron IIA Tel es-Safi, iron production debris (radiocarbon dated to the late 10th-9th c. BC) was found with a crucible for making leaded tin bronze (Eliyahu-Behar, et al., 2012). At Tayinat, Early Iron Age iron and copper production was also reported from a single workshop (Roames, 2011). However, in the latter case, identification of production residues was based solely on macroscopic morphology and XRF analysis of the (corroded) surface, and should be considered preliminary.

Second, iron production remains at different sites differ significantly in their quantity and character (Yahalom-Mack and Eliyahu-Behar, 2015:294-295). Whether these differences reflect different stages in the *chaîne opératoire*, multiple co-existing technological styles (cf. Lechtman, 1977), different taphonomic processes at each site, or a combination of the above—remains somewhat unclear. Veldhuijzen's excavations of 10th-9th c. BC iron smelting remains at the site of Tell Hammeh suggest that the metal production occurred during a break in permanent habitation at the site. Quantities of iron production slag at Tell Hammeh exceed those found at other iron production sites in the southern Levant. 700 kg of slag were recovered during the excavation of an estimated 5-10% of the total area dedicated to production. (Veldhuijzen and

Rehren, 2007:192-193). At Tel Beth Shemesh, iron metallurgical activities were restricted to secondary smithing, suggesting a segmentation of production activities between urban and non-urban contexts. (Veldhuijzen and Rehren, 2007:198-199; Veldhuijzen, 2009).

Other research has advanced the case for iron smelting at urban centers, though the quantity and character of this smelting debris differed from that at Tell Hammeh. The first such argument was based primarily on the macro-morphology and chemical analysis of a piece of slag from Tel es-Safi (Eliyahu-Behar, et al., 2012:261-264). However, distinguishing smelting and smithing slags based on chemical data is problematic, as myriad other factors affect slag composition (see Section 2.1). Also, there may be significant diversity in the macroscopic appearance of iron slags, even those from the same process (Miller and Killick, 2004:27-28). Subsequent analysis of other iron production remains—mostly from Hazor (Iron IIA and IIB), but also from Tel Rehov, and Tel Beer Sheba—provided a stronger case for iron smelting in an urban context (Eliyahu-Behar, et al., 2013). At Hazor, a fragment of hematite iron ore was found in association with corroded iron fragments and slag cakes. Microstructural analyses of the slag cakes identified metallic iron in the process of being chemically reduced from iron oxide. Taken together, the evidence from these sites provides a reasonable, though perhaps not definitive, argument for iron smelting. Slag adhering to the bloom may liquify and flow into the hearth during primary smithing. As a result, primary smithing slags might still contain small pieces of metallic iron and partially reduced ore that failed to consolidate with the bloom, and might be very difficult to distinguish from a smelting slag (Greenfield and Miller, 2004:1521; Miller and Killick, 2004:31).

These ambiguities highlight the importance of laying out interpretive criteria for identifying different stages iron production. Similar discussions for iron production in Africa

(Miller and Killick, 2004) and historic North America (Gordon, 1997) provide a good starting point, but it is important to develop these criteria for the Iron Age Near East. The earlier research on iron production in the Levant, discussed above, has begun this process, but it is essential that more iron metallurgical remains be analyzed to generate a meaningful corpus of information.

Distinguishing stages of iron production has important ramifications for understanding the relative organization of iron and copper/bronze production. Because comparisons of these two metal industries are a major element of many discussions about the spread of iron (Mirau, 1997; Snodgrass, 1980:336-337; Veldhuijzen, 2012:238), understanding where and in what social contexts these metals were produced is important. Although there is evidence for copper smelting far from ore deposits during the Chalcolithic period (Golden, et al., 2001; Levy and Shalev, 1989:365; Shugar, 2003), there is little evidence for it at large urban in the Early Bronze Age and subsequent periods. If metalworkers imported raw copper from elsewhere, but were able to smelt iron locally, this pattern of production would give credence to the theory that iron spread because it was more accessible to communities far from copper ore deposits.

Identification of production debris is important since the broad geological availability of iron ore is not in itself proof that people exploited those deposits. The analysis of metallurgical remains from Iron Age Ashkelon offers an opportunity to investigate questions about the organization of Levantine metal production, and by extension, the expansion of iron production in the Iron II period.

2. Criteria for Distinguishing Metal Production Stages

2.1. Iron Production

128

129 Early iron production relied on the bloomery smelting process. Because of the high
130 melting temperature of iron, the product of iron smelting was not molten iron metal, but a spongy
131 mass of solid iron and slag known as a bloom. Primary smithing consolidated the bloom,
132 squeezing out most of the interstitial slag and producing a mass of partly refined metal that
133 would have been easier to handle in transport. Secondary smithing refers to the process of
134 forging finished goods from the billet. All of these stages produced metallurgical slag and other
135 production debris, which are typically discarded in the workshop itself or nearby.

136 Macroscopic examination of the quantity and character of slag and other production
137 debris is the essential first step in identifying these different activities archaeologically. Iron
138 smelting typically produces greater quantities of slag than iron smithing. Iron smelting slags are
139 formed from melted gangue (ore host rock), unreduced ore, furnace material, and fuel ash and
140 occasionally a deliberately added flux, whereas smithing slags are derived from smelting slag
141 adhering to or trapped within the bloom, oxidized flakes of iron called hammerscale, and perhaps
142 some hearth material. However, absolute quantities of slag are not always a reliable indicator of
143 production stage. For example, in urban settings where space was at a premium, craftspeople
144 may have frequently removed debris from their working areas, sometimes to multiple locations.
145 On the other hand, in rural settings where space was more abundant, slag may have accumulated
146 next to the working areas. Thus the archaeometallurgical record can be misleading with regards
147 to the interpretations of original scale and location of production.

148 Tap slags are often considered to be a diagnostic feature of iron smelting (Yahalom-Mack
149 and Eliyahu-Behar, 2015:294). However, small dribbles or flows of slag, mimicking true tap
150 slags, may form within a smelting furnace, so it is important to examine possible tap slags

151 closely. Microscopic crusts of iron oxide at the surface of a slag, indicating a rapid cooling and a
152 change of redox conditions, is characteristic of true tap slags (Miller and Killick, 2004:24).

153 Bulk chemistry is a poor method for distinguishing between smelting and smithing slags.
154 A close examination of slag mineralogy and microstructures through optical and scanning
155 electron microscopy is essential. Relative proportions of wüstite (FeO) and magnetite (Fe₃O₄)
156 indicate the atmospheric conditions under which the slag formed, with the former indicating
157 more reducing conditions than the latter. Smithing hearths generally have more oxidizing and/or
158 more variable conditions, while smelting furnaces are more reducing. However, it is important to
159 note that redox conditions varied within early hearths and furnaces, and these slags formed in
160 non-equilibrium environments. Thus, while iron oxide states should be considered, this
161 information alone should not be used to distinguish between smelting and smithing processes.

162 The presence of metallic iron is another important feature. Iron smelting slags, especially
163 furnace slags, typically contain small particles or aggregates of iron that failed to coalesce into
164 the bloom during smelting. By definition, iron ore is not reduced to metal in a smithing hearth.
165 The only way for metallic iron to make its way into a smithing slag is for fragments of bloom (or
166 iron metal aggregates in slag adhering within the bloom) to fall into the smithing hearth while
167 avoiding oxidation (Miller and Killick, 2004:31). Particles of iron metal have been observed in
168 smithing slags, notably in association with magnetite and wüstite, which are indicate highly
169 variable redox conditions inconsistent with a smelting slag (Rehren, 2012). Recent investigations
170 by Soulignac (2017) illustrate the mineralogical diversity found in smithing slags, showing that
171 metallic iron does appear in slags formed during lengthy, high-temperature smithing operations.

172 The presence of partially-reacted ore fragments is another diagnostic feature of iron
173 smelting slags. However, most common iron ores are iron oxides, which are ubiquitous as

freshly formed phases (usually wüstite and/or magnetite) and as post-depositional alternation (iron hydroxides) in all kinds of iron production slags. Therefore, identifying primary additions to the smelt requires careful interpretation of microstructures (for analogous cases using micromorphology to identify primary additions, see Erb-Satullo, et al., 2015; Killick and Miller, 2014:247).

The preceding discussion illustrates the challenges of distinguishing smelting and smithing at urban sites where debris may have been cleaned up or re-deposited. A reconstruction of the various kinds of metal production taking place at a site must consider the assemblage as a whole, making clear what interpretations are certain, and which ones are only probable.

2.2. Copper production

Distinguishing copper smelting debris from refining and casting debris is usually more straightforward. The presence of partially reacted ore fragments or gangue (i.e. host rock) minerals trapped in slag is diagnostic of smelting. Chemical compositions may also indicate smelting if there are large contributions from certain elements that could only have come from the ore or gangue minerals. As with iron metallurgy, quantities of slag associated with smelting are generally much larger than those associated with secondary refining, casting, and forging operations, though the same taphonomic considerations apply. Slag is produced in refining processes when a flux is mixed with raw copper, lowering the iron content and making it more suitable for working (Craddock and Meeks, 1987:192). Copper refining slags produced during this process will reflect more oxidizing conditions. If the original ore deposit contained copper or iron sulfides, one would typically expect to find more copper sulfide in a smelting slag than a

slag produced later on in the process. However the relative quantities will be heavily affected by the sulfide content of the ore used, and the absence of sulfides may simply mean that the ore did not contain any.

3. Metal Production Debris in Iron II Ashkelon

Metallurgical debris from the Iron II layers at Ashkelon provides an ideal opportunity to explore the *chaîne opératoire* of copper and iron metallurgy in a settlement context. Ashkelon was a Philistine urban center and port city throughout the Iron Age, and has been excavated by the Leon Levy Expedition to Ashkelon over the last 30 years. All of the metallurgical samples discussed here come from Grid 38, the only excavation area at Ashkelon with substantial 8th-9th century BC remains. The area is best characterized as a domestic quarter from the arrival of the Philistines at the onset of the Iron I in the early 12th century BC (Aja, 2009) until its conversion into a winery in the 7th century BC (Stager, et al., 2011). The metal production remains discussed here include all of the metallurgical samples recovered from phases 15 (Iron IIB, 8th century BC) and 16 (10th/9th century BC) (**Table 1**). Whereas a few additional samples were mentioned in field records, these could not be located by the authors for analysis. The samples originate largely from phase 15, with one sample, A20, originating from phase 16 or 17 (**Fig. 2**). Some of the metallurgical samples come from secondary contexts, mixed in with either mudbrick material or foundational cobbles and incorporated into wall construction. Of 23 samples, six (A3, A7, A12, A20, A14 and A15) fall into this category. As such, the original context of these samples is earlier than the contexts in which they were discovered, possibly as early as the late 11th/early 10th century BC (see Van Beek and Van Beek, 2008:131 on artifacts in mud brick constructions).

Other samples come from clear 8th century BC contexts. Three samples (A1, A2, and A9) were found in large silos accompanied by a predominantly 8th century ceramic assemblage. Three additional samples (A17, A21, and A23) were found in the fill of a similar silo, best associated with activities taking place in the nearby houses, where additional samples were found (A16, A19, A11, and A13). Sample A13 was found in an occupational accumulation on a courtyard surface, while other samples were found as part of a leveling fill on top of this surface, and could be plausibly associated with the same area. No unequivocal pyrotechnical installations were discerned, but these installations can be quite ephemeral and difficult to identify (see Eliyahu-Behar, et al., 2012).

A second concentration was found in building 91 in the northern extent of the excavation trench, adjacent to the first silo mentioned above. Sample A5 was found on a nearby floor, and two additional samples (A4 and A6) in a nearby fill.

Finally, a crucible rim (A18) was found inside a circular walled feature, preliminarily identified as a tabun, within a multi-function courtyard. This feature is probably too large (c. 1 m in diameter) to be a smelting furnace, but the presence of metallurgical debris suggests that it could conceivably be metallurgical installation relating to a production stage not requiring highly reducing conditions.

Despite the secondary context of most of the samples, these residues can still provide a useful picture of metal production at Iron II Ashkelon. Especially in the case of pit and leveling fills, the material deposited likely originated from the immediate vicinity, and thus can be associated with activities conducted in the surrounding buildings. It is both impractical and unlikely that material was brought from long distances for these filling events. Thus, even if the final contexts of these slags are secondary, they are indicative of metallurgical activity in nearby

domestic neighborhoods during the 8th century BC. Samples from inside the brick material of walls, especially small samples like A20, may have come from farther away, but brick material is generally quarried from as close to the building site as possible, to avoid costly and time-consuming transportation (Van Beek and Van Beek, 2008:130-131).

4. Analytical Methods

In order to determine what stages of metal production were carried out at Ashkelon, slags and slagged crucible fragments were analyzed using reflected light optical microscopy and scanning electron microscopy with an energy dispersive X-ray detector (SEM-EDS). SEM-EDS analyses were carried out with an Oxford Instrument INCA X-Sight EDS system at the Museum of Fine Arts in Boston. Mineralogical identifications were based on optical properties, EDS chemical analyses, and phase morphologies. Bulk chemical analyses were carried out by scanning the beam over a defined area, avoiding as much as possible corroded areas, voids, and partially reacted inclusions. For each sample, at least four different area analyses were averaged to account for intra-sample variability.

5. Analytical Results

5.1. Iron Metallurgical Debris

A majority of the samples relate to iron metallurgy (**Table 2**). With this group, several different types of slag were distinguished. Slag cakes and slag cake fragments were one of the

most common types of debris (**Fig. 3**). While only the clearly identifiable examples were labeled as such in **Table 2**, it is likely that most of the smaller fragments fall into this category as well. Slag cakes often form at the base of the hearth (in the case of smithing) or furnace (in the case of smelting), and as discussed above, it is often difficult to distinguish between them based on macroscopic characteristics alone (e.g. Veldhuijzen, 2005:174). Nonetheless, there is some macroscopic variability among Ashkelon slag cakes, suggesting different activities. Two of the largest examples (A3 and A5) are thick and had a rough surface covered in heavy orange corrosion. In contrast, sample A15 has a smooth upper surface with only spots of orange corrosion.

Microscopically, all slag cake samples were dominated by a combination of iron silicates (mostly the olivines, fayalite and kirschsteinite) and iron oxides and lack any copper-bearing phases. Still, there were important microscopic differences. Some samples formed in atmospheric conditions that were both more oxidizing and more variable than others (**Fig. 4**). These samples contain wüstite in the process of transforming into magnetite, and magnetite preserving relict wüstite morphologies. Such heterogeneous conditions are more consistent with a smithing hearth than a smelting furnace. Moreover, oblong and linear clusters of iron oxides observed in A4 are likely flakes of hammer scale that made their way into the slag, providing further evidence of smithing (**Fig. 4A, B**) (cf. Eliyahu-Behar, et al., 2013).

In contrast, the mineralogy of other iron slags suggest they formed under altogether different conditions. In this group of samples, wüstite is the dominant iron oxide. Metallic iron and corroded iron metal are much more common in these slags (**Fig. 5**). Areas of now-corroded iron metal were identified based on microstructural analyses. Small islands of uncorroded metal in the midst of larger corroded areas provide clues as to the former metallic character of these

phases (**Fig. 5A, B**). In other cases, relict steel microstructures are visible (**Fig. 5C**). While distinguishing partially reacted iron ore, corroded metal, and post-depositional precipitates is sometimes challenging, partially reacted inclusions of iron ore were also identified. One example in sample A17 (**Fig. 5D**), shows iron metal and corroded iron metal surrounding a porous fragment of iron ore. The microstructure of this fragment, and the surrounding metal, makes it clear that it is not the result of corrosion or post-depositional infilling of voids in the slag.

It is important to note that there are no consistent chemical differences between samples formed under more oxidizing or mixed atmospheres, and those formed under more reducing conditions (**Table 3**). The key differences between samples associated with the later stages of smithing and those that result from smelting are mineralogical and morphological, *not* chemical.

In addition to slag cakes and cake fragments, small fragments of tap slags are also present in the assemblage. Samples A1, A7, and A10 (**Fig. 3**) display classic macroscopic characteristics of tap slags: flow textures, and traces of contact, but not reaction, with the surface onto which it flowed. Rapidly cooling tap slags generally do not fuse with these surfaces. Microscopically, the tap slag contained mostly fayalite crystals with fine dendrites of wüstite crystallizing in the interstices (**Fig. 6A**). Metallic iron was noted in one of the two samples, but not in large quantities. As is common with tap slags, thin skins of iron oxide precipitated between flows and along surfaces exposed to the air outside the furnace (**Fig. 6B**).

A third piece of slag (A1) was tentatively identified as a tap slag, but its appearance makes it clear that it remained highly viscous (**Fig. 3**). A2, a non-joining fragment also found with A1, has a very similar microstructure and chemical composition. Both samples consist almost entirely of wüstite with very little interstitial material (**Fig. 7**), and therefore have chemical compositions very rich in iron (**Table 3**). Metallic iron is present in both samples.

Intriguingly, prills of calcium-rich material were noted, paralleling similar features reported in iron production remains elsewhere in the southern Levant (Eliyahu-Behar, et al., 2013). Reaction halos where the calcium-rich material melted into the slag make it clear that these prills are not the result of post-depositional infilling of gas bubbles. The best interpretation of sample A1 (and perhaps A2, though its macromorphology is unclear) is that it is partly reacted ore that was tapped too early in a smelt.

The final type of iron production slag was sample A14, a silica-rich slag dominated by rounded, partially reacted grains of quartz sand, with numerous small particles of metallic iron (**Fig. 8**). As an isolated sample, it is difficult to interpret whether this slag reflects an intentional process (perhaps use of beach sand as a flux) or merely the accidental mixing of sand and slag. Two other silica-rich slags, A22 and A23, are probably related to iron production, but their identification is less certain. These two samples contain no copper-bearing phases, and no metallic iron. Given their association with other metallurgical debris and their chemical and microstructural similarity to A14, they are probably metallurgical in origin. If so, they are likely connected with iron production, as one would expect slags associated with copper metallurgy to have some trace of copper in them.

5.2. Copper Metallurgical Debris

Four of the samples analyzed (A18, A19, A20, and A21) relate to copper metallurgy. Samples A18 and A19 are clearly associated with crucible processes. The former is a crucible rim with small droplets of slag and copper minerals adhering to the surface, while the latter is a lump of slag that cooled over the rim of a crucible, traces of which adhere to the sample. Sample

A20 is a small dribble of slag. A21 is a small broken fragment of slag too small to classify macroscopically.

Sample A19 is clearly related to the secondary processing of raw copper to reduce its iron content through fluxing, probably immediately prior to casting (**Fig. 9A**). The presence of numerous partially-reacted quartz grains points to intentional fluxing with beach sand gathered nearby (see Craddock and Meeks, 1987:192). None of these quartz grains have copper minerals attached to them, as one would expect if the quartz was a gangue mineral added with ore. Abundant cuprite, delafossite, and magnetite attest to oxidizing conditions, consistent with refining rather than smelting. Copper prills are very common in the sample, but sulfides were not identified. Droplets of slag and copper-bearing minerals were identified adhering to the surface of sample A18. The copper-bearing minerals (a mixture of oxides, carbonates, and chlorides) are either post-deposition corrosion or oxidation during a secondary copper refining and/or casting process. A tiny droplet of slag found adhering to the surface consists mostly of very fine dendrites of iron oxide (probably wüstite), and minute ($\leq 10\ \mu\text{m}$) prills of copper-iron sulfide.

A20 is a mostly glassy slag containing prills of both copper sulfide and copper metal (**Fig. 9B**). Very fine crystals are apparent in the glassy matrix, but their small size prevents definitive identification. Most intriguingly, this slag contains a significant amount of manganese (8.3 oxide wt. %) and phosphorous (17.2 oxide wt.%) (**Table 3**). The high quantities of these elements, which derive from the ore deposit, mark this sample as a product of copper smelting. Manganese is a known component of smelting slags in numerous regions of the eastern Mediterranean, including both the Timna and Faynan regions as well as the island of Cyprus and the Sinai peninsula (Bachmann, 1980; Bachmann, 1982; Hauptmann, 2007:180-199; Koucky and Steinberg, 1982). The iron and manganese content of A20 matches the composition of smelting

slags from Timna and the Sinai more than those from Faynan (Hauptmann, 2007:180). As manganese is largely incorporated into the slag, rather than the metal, during smelting (Tylecote, et al., 1977:324), secondary copper refining slags, produced by re-melting the metal and fluxing with sand, should contain less Mn than smelting slags. The high phosphorous is also probably ore-derived, as phosphates are noted in the Dolomite-Limestone-Shale formation at Faynan and the Timna formation at Timna (Hauptmann, 2007:66, 70).

Sample A21 consists mostly of wüstite and fayalite that contain instances of prills rich in varying amounts of iron, copper, and arsenic (**Fig. 10**). At least one of these prills contains iron and arsenic concentrations high enough that it borders on the composition of speiss, an intermetallic compound that may have been intentionally produced in some ancient contexts (Rehren, et al., 2012; Thornton, et al., 2009). Abundant wüstite dendrites (over a much larger area than the minute slag droplet in A18) suggest strong reducing conditions. Area analyses contained virtually no detectable copper (**Table 3**). While area analyses were not intentionally chosen to avoid prills, the areas analyzed did not encompass the largest instances. Further examination revealed that the prills are restricted to certain areas of the sample. These results show that the overall copper content of the slag is quite low. Despite a wüstite-dominated microstructure that matches iron slags in the assemblage quite well, the presence of copper-bearing phases—however minor—suggests some connection to copper-base metallurgy.

6. Discussion

The iron production slags found in Iron Age contexts at Ashkelon, though small in number, attest to an array of production activities. Clear distinctions can be made between slags

formed in more oxidizing conditions, and those formed under highly reducing conditions. It is likely that these different slags represent distinct stages in the sequence of production, from smelting to primary and secondary smithing. As noted in section 2.1, however, similarities between slags, particularly from adjacent stages in the production sequence, make interpretations of individual slags somewhat tentative (**Table 2**). We must therefore consider the arguments for smelting and smithing at Ashkelon from the perspective of the assemblage as a whole.

The case for smelting is based on several aspects of the iron production assemblage. First, the identification of a partially reacted ore inclusion surrounded by particles of reduced iron in sample A17 (**Fig. 5D**) and perhaps A5 is strong evidence for smelting. The presence of at least two and perhaps as many as four pieces of tap slag leads to a similar conclusion, as slag tapping is not part of the smithing process. The viscous tap slag morphology and high wüstite content of sample A1 are best explained as fused ore accidentally tapped too early from the smelting furnace. The calcium-rich material identified in various stages of reaction with the melt in samples A1 and A2 is probably derived from the ore. Finally, the presence of metallic iron and corroded metallic iron pseudomorphs, particularly those with microstructures suggesting recent reduction from wüstite, is also consistent with smelting.

An alternative interpretation—one in which smelting did not take place at Ashkelon—might suggest that slags such as A3 and A5 are the result of primary smithing rather than smelting. Ethnographic research does show that metallic iron can appear in smithing slags, particularly those from extended, high-temperature forging processes (Soulignac, 2017). Consider the reverse scalloped edges and iron oxide crusts on the relict steel microstructures in sample A8 (**Fig. 5C**). This micromorphology might be the result of small piece of iron breaking off during smithing, falling into the hearth, and beginning to oxidize. Alternatively, it could

404 simply be the result of particles of reduced iron travelling into a slightly more oxidizing
405 atmosphere in a smelting furnace. Still, a “smithing only” interpretation would not account for
406 the microstructures interpreted as partially reduced iron ore fragment in A17 and possibly A5.
407 The tap slags are even harder to explain in this scenario, and would have to be rationalized as
408 accidental flows of slag from the smithing hearth. This explanation is unsatisfactory, since the
409 smithing operations do not produce large quantities of fluid, homogeneous slag that might
410 accidentally overflow the hearth. Finally, the evidence of primary smithing at Tell Hammeh, a
411 site with unequivocal evidence of smelting (Veldhuijzen, 2005:186-188) suggests that primary
412 smithing and smelting occurred at the same sites. In sum, an argument against smelting at
413 Ashkelon requires a series of unlikely assumptions and difficult rationalizations of the available
414 data, whereas the alternative—that smelting did take place relatively close to where the slags
415 were found—is a more reasonable conclusion.

416 While the “smithing only” argument is problematic, there is good evidence that primary
417 and/or secondary smithing did take place at Ashkelon. The instances of hammerscale dissolving
418 into the slag are particularly diagnostic. The diminished presence of metallic iron, and the
419 presence of magnetite also points to more oxidizing conditions consistent with smithing, though
420 this is not necessarily definitive, as smelting furnaces can have heterogeneous redox conditions.
421 The correspondence between macroscopic and microscopic characteristics, as in the case of the
422 smooth surfaced slag cake A15, also supports the hypothesis of multiple distinct metallurgical
423 activities (**Figs. 3 and 4C, D**). This slag cake is likely a smithing hearth bottom, while the
424 thicker, rougher cakes probably relate to smelting (e.g. A3). Still, metallic iron does occasionally
425 appear in smithing slags in this assemblage (**Fig. 4C, Table 2**) as well as others (Greenfield and
426 Miller, 2004:1521; Rehren, 2012). Wüstite can also appear in smithing cakes (Veldhuijzen and

Rehren, 2007:198), just as magnetite may form in some more oxidizing areas of a smelting furnace. Yet despite these caveats and qualifications when discussing a single sample, the assemblage as a whole makes it clear that multiple stages of iron production occurred at the site.

The smaller number of samples of copper metallurgical debris offers a more limited window into these activities at Ashkelon. Sample A19 is strongly indicative of copper refining. The addition of beach sand into the reaction vessel with molten copper would have reduced the iron content of copper through preferential oxidation of iron, making it more suitable for working (Craddock and Meeks, 1987:188, 192). The slag would have formed a protective layer, preventing further loss of copper through oxidation. The crucible rim with minute slag droplets and copper mineral, A18, is probably from the same process.

The broader significance of samples A20 and A21 is harder to assess. Sample A20's identification as a smelting slag is clear from its chemical and mineralogical composition, yet its small size and secondary context make it much harder to argue that copper smelting occurred at Ashkelon in the Iron Age. Perhaps the slag adhered to a copper ingot as it was taken from a distant smelting source (see similar reasoning in a discussion of crucible slags in Bachmann, 1980:116). Sample A21 is also unusual in several ways. The copper-containing prills point to copper-base metallurgy, but the high iron content of the prills and the highly reducing conditions are unusual for copper metallurgy. The absence of more than one sample of this type makes its interpretation challenging. One possibility is that the sample came from a copper smelt that became excessively reducing. A more remote possibility is that it derives from an iron metallurgical process that somehow became contaminated with copper and arsenic, but with only one sample of this type, this possibility remains conjectural. Hence, a provisional association with copper-base metallurgy is justified, until further work reveals whether A21 is merely

reflective of heterogeneity within normal copper-base metallurgy, or indicative of a different technological process.

7. Conclusions

Macro- and micromorphological observations, slag chemistry, and mineralogy suggest that several different stages of iron production occurred at Ashkelon. It is likely that metallurgical activities occurred in or near the structures excavated in Grid 38. The mix of residues associated with various stages of the *chaîne opératoire* of copper and iron production indicate that both copper and iron objects were produced in relatively close proximity, perhaps even in the same workshop. However, for reasons discussed above, sample A20 is not enough to overturn the general observation that Iron Age copper smelting, unlike iron smelting, seems to have taken place away from these coastal cities.

Recent scholarship has advanced the idea that multiple different iron smelting technologies coexisted in the Iron II period, perhaps reflecting the early period of innovation and experimentation (Yahalom-Mack and Eliyahu-Behar, 2015:300). Yahalom-Mack and Eliyahu-Behar are correct to note significant quantitative and qualitative differences between the production debris found at Hazor and Tell Hammeh. Yet these contrasting archaeological assemblages may not reflect differences in smelting technologies (e.g. non-tapping pit-smelting vs. tapping furnaces), as much as differences in the scale and context of production. At Ashkelon, finds of tap slag, a type not found at Tel es-Safi or Hazor, draw a link between the techniques seen at non-urban Tell Hammeh and urban sites to the west. On the other hand, Ca-

rich prills noted in the Ashkelon slags echo those seen in slags at Hazor (Eliyahu-Behar, et al., 2013). As a whole, the Ashkelon assemblage may suggest a greater unity in iron metallurgical techniques. Regardless, in discussions about distinct smelting traditions, we must be cautious in interpreting the partial assemblages at Ashkelon, Hazor, and Tel es-Safi.

As archaeologists become increasingly adept at identifying and analyzing ephemeral traces of metal production, careful reconstruction of the various stages of production present at different locales is vital. Without an accurate understanding of where different iron and copper-alloy production activities took place, models of innovation and technological change in the Iron Age remain purely conjectural. Analyses of metal production debris at Ashkelon illustrate the challenges facing these technological reconstructions, while demonstrating that even small assemblages of debris can furnish useful information.

Acknowledgements

The authors would like to thank Lawrence Stager and Daniel Master, the directors of the Leon Levy Expedition to Ashkelon, who allowed us to access and publish this material. The excavations at Ashkelon are funded by the generous support of the Shelby White and Leon Levy Foundation. Special thanks to Richard Newman and the Boston Museum of Fine Arts Scientific Research Lab, who provided access to the scanning electron microscope and guidance in its use. Discussions with David Killick and Erez Ben-Yosef were helpful in refining our interpretations of the slags. Detailed comments by two anonymous reviewers greatly strengthened the paper.

Figures

Figure 1. Map of the Levant with sites mentioned in the text. Elevation data: GTOPO30.

1.5 Column Size

Figure 2. Plan of Grid 38 Excavations (Phase 15) showing loci with copper and iron production debris. A20, found inside a Phase 16/17 wall, is not shown.

Double column size

Figure 3. Types of metal production debris found at Ashkelon.

Double column size

Figure 4. Optical photomicrographs showing evidence of iron smithing. A and B show elongated clusters of iron oxides that are flakes of hammerscale dissolving into the slag. Note presence of both wüstite dendrites and equiaxed magnetite, illustrating variable reducing conditions that are generally more oxidizing than those within which the wüstite-dominated smelting slags were formed. A single isolated inclusion of metallic iron (C) was observed in sample A15, but the rest of the sample is dominated by magnetite (D), indicating redox conditions unfavorable for the reduction of iron metal. Unless otherwise stated, all optical photomicrographs were taken under plane polarized light.

Double column size

Figure 5. Optical photomicrographs of metallic iron and partially reacted ore fragments. A. Small islands of iron metal suggest that much of the light grey iron oxide cluster is in fact corroded iron metal. B. Particles of metallic iron amid larger clusters of corroded iron metal, accompanied by wüstite phases. C. Relict ferrite and pearlite microstructures preserved in iron corrosion. D. Partially reacted iron ore fragment with iron metal forming at its edges. Key: Fe-iron metal; Fe Ore-partially reacted iron ore; (Fe)-corroded iron metal; (Fr-Prl)-relict ferrite and pearlite structures preserved in corroded metal.

Double column size

Figure 6. Optical photomicrographs of tap slag microstructures. Sample A10 is characterized by fayalite and interstitial wüstite dendrites. A tapping band, which forms at slag air interfaces and between separate flows of slag, is visible in sample A7.

Double column size

Figure 7. Backscatter SEM images of iron smelting slags with calcium-rich prills. Samples consist of very high quantities of wüstite, with prills of calcium-rich material. Reaction halos clearly show that calcium-rich materials were not the result of post-depositional precipitation of calcium carbonate in previously-vacant gas bubbles.

Double column size

Figure 8. Photo and optical microscope image of sample A14. The microstructure of the samples is characterized by partially reacted quartz inclusions (Qz) and small particles of metallic iron

(Fe) within a glassy matrix. Small amounts of magnetite (not shown) were occasionally observed elsewhere in the sample.

Double column size

Figure 9. SEM backscatter images of copper production slags. A. Copper processing slag with quartz sand inclusions (Qz), bright feathery cuprite dendrites (Cup), the iron oxide magnetite (Fe-Ox), delafossite (Dlf) and copper metal (Cu). B. Copper smelting slag with prills of copper metal (Cu) and copper sulfide (Cu-S).

Double column size

Figure 10. Optical and scanning electron microscope images of Sample A21, along with EDS spectrum of prill and photo of the sample. SEM image is a higher magnification image of the same area prill in the optical microscope image.

Double column size

558 **Tables**

Sample #	Reg #	Prod. Type	Context Description	Phase
A1	5025	Fe	Pit/Silo	15
A2	5025	Fe	Pit/Silo	15
A3	11743	Fe	Wall makeup	15
A4	12294	Fe	Leveling fill	15
A5	12301	Fe	Floor	15
A6	12329	Fe	Leveling fill	15
A7	51157	Fe	Wall makeup	15
A8	52985	Fe	Leveling fill	15
A9	53738	Fe	Pit	15
A10	57405	Fe	Leveling fill	15
A11	62452	Fe	Leveling fill	15
A12	62722	Fe	Wall makeup	15
A13	62753	Fe	Occupational accumulation on floor	15
A14	63124	Fe	Wall makeup	15
A15	63124	Fe	Wall makeup	15
A16	66540	Fe	Leveling fill	15
A17	67823	Fe	Pit fill	15
A18	45920	Cu	Fill in tabun	15
A19	62451	Cu	Leveling fill	15
A20	63003	Cu	Wall makeup	17/16
A21	67309	Cu?	Pit fill	15
A22	67208	Fe?	Mixed fill	16/15
A23	67398	Fe?	Pit fill	15

559 Table 1. List of samples analyzed, with information about production type, context, and phase
560 assignments. Leveling fill refers to leveling activities in preparation for Phase 14 constructions,
561 but the artifacts contained in them belong to Phase 15.

Sample #	Reg. #	Macroscopic Morphology	Metallic Iron?	Dominant Iron Oxide	Stage of Iron Production
A1	5025	Tap slag (v. viscous)	XX	Wüstite	Smelting Slag
A2	5025	Small fragment	X	Wüstite	Smelting Slag
A3	11743	Slag cake	—	Wüstite	Probable Smelting Slag
A4	12294	Small fragment	—	Magnetite/Wüstite	Probable Smithing Slag
A5	12301	Slag cake	XX	Wüstite	Smelting Slag
A6	12329	Small fragment	X	Wüstite (mostly interstitial)	Uncertain
A7	51157	Tap slag	—	Wüstite (interstitial)	Smelting Slag
A8	52985	Small fragment	XX	Wüstite	Uncertain
A9	53738	Small fragment	XX	Wüstite	Probable Smelting Slag
A10	57405	Tap slag	X	Wüstite (interstitial)	Smelting Slag
A11	62452	Small fragment	X	Wüstite	Possible Smelting Slag
A12	62722	Slag cake	—	Magnetite	Possible Smithing Slag
A13	62753	Small fragment	XX	Minimal Fe-Oxide	Probable Smelting Slag
A14	63124	Silica-rich slag	XX	Minimal Fe-Oxide	Possible smelting slag
A15	63124	Slag cake	X (1 instance)	Magnetite	Smithing (probably secondary)
A16	66540	Small fragment	X	Wüstite	Probable smelting slag
A17	67823	Small fragment	XX	Wüstite	Smelting Slag
A22	67208	Small fragment	—	Minimal Fe-Oxide	Uncertain
A23	67398	Small fragment	—	Minimal Fe-Oxide	Uncertain

563

564 Table 2. Mineralogy and interpretation of iron production slags. Rough quantities of metallic
565 iron are recorded as present in significant quantities (XX), present in small quantities (X) or not
566 identified in the sample (—). This designation also counts clear instances of corroded metallic
567 iron. Description of dominant iron oxide profile excludes corrosion products and occasional
568 unreacted ore grains. The most likely interpretations of production stage are unqualified,
569 followed by “probable” and “possible” in declining certainty.

570

Sample #	Prod. Type	Reg #	Na ₂ O	MgO	Al ₂ O ₃	SiO ₂	P ₂ O ₅	SO ₂	Cl	K ₂ O	CaO	TiO ₂	MnO	FeO	CuO	ZnO	BaO	As ₂ O ₃	PbO
A1	Fe	5025	0.3	0.6	0.6	6.6	bdl	bdl	bdl	0.3	5.2	bdl	bdl	86.5	bdl	nm	bdl	nm	nm
A2	Fe	5025	0.4	3.5	1.4	15.3	0.9	bdl	bdl	0.9	11.6	bdl	bdl	66.0	bdl	nm	bdl	nm	nm
A3	Fe	11743	0.6	0.7	4.5	23.0	0.4	0.4	bdl	1.5	3.9	bdl	bdl	64.5	bdl	nm	0.4	nm	nm
A4	Fe	12294	0.9	1.1	2.9	28.0	0.3	bdl	bdl	1.2	8.3	bdl	bdl	57.4	bdl	nm	bdl	nm	nm
A5	Fe	12301	0.4	0.8	3.2	14.7	bdl	bdl	bdl	1.0	2.6	bdl	1.1	76.3	bdl	nm	bdl	nm	nm
A6	Fe	12329	1.4	0.4	4.1	30.3	0.8	bdl	bdl	1.4	6.4	bdl	bdl	55.2	bdl	nm	bdl	nm	nm
A7	Fe	51157	0.6	0.6	3.8	32.9	0.3	bdl	bdl	1.4	5.1	0.3	bdl	55.0	bdl	nm	bdl	nm	nm
A8	Fe	52985	0.6	0.8	3.2	21.3	0.3	bdl	bdl	1.3	8.9	bdl	bdl	63.5	bdl	nm	bdl	nm	nm
A9	Fe	53738	0.5	2.9	2.8	33.6	0.3	bdl	bdl	0.7	4.9	bdl	bdl	54.5	bdl	nm	bdl	nm	nm
A10	Fe	57405	0.6	0.5	5.0	32.3	0.5	bdl	bdl	1.9	5.1	0.3	bdl	53.9	bdl	nm	bdl	nm	nm
A11	Fe	62452	0.6	1.2	7.6	21.4	0.9	bdl	bdl	2.0	6.0	0.4	bdl	59.8	bdl	nm	bdl	nm	nm
A12	Fe	62722	1.2	0.6	5.6	34.1	0.5	bdl	bdl	2.2	6.0	0.4	bdl	49.3	bdl	nm	bdl	nm	nm
A13	Fe	62753	0.8	0.5	5.5	37.4	0.8	bdl	bdl	1.5	6.0	0.3	bdl	47.1	bdl	nm	bdl	nm	nm
A14	Fe	63124	0.6	1.2	7.0	56.3	0.4	bdl	bdl	2.2	9.8	0.7	bdl	21.7	bdl	nm	bdl	nm	nm
A15	Fe	63124	0.6	0.6	3.2	39.8	0.5	bdl	bdl	1.7	7.0	bdl	bdl	46.6	bdl	nm	bdl	nm	nm
A16	Fe	66540	0.5	0.7	5.5	26.4	1.3	bdl	bdl	1.7	4.3	bdl	bdl	59.6	bdl	nm	bdl	nm	nm
A17	Fe	67823	0.4	0.8	1.6	26.4	0.3	bdl	bdl	0.8	2.0	bdl	bdl	67.6	bdl	nm	bdl	nm	nm
A18	Cu	45920	bdl	0.6	3.2	16.4	bdl	1.7	bdl	0.5	1.7	bdl	bdl	72.4	3.4	nm	bdl	nm	nm
A19	Cu	62451	0.3	1.3	5.9	46.1	0.6	bdl	bdl	1.3	10.0	0.5	bdl	15.3	18.2	0.3	bdl	0.3	nm
A20	Cu	63003	0.7	1.3	2.7	23.2	17.2	0.3	bdl	1.6	7.9	bdl	8.2	34.8	0.8	nm	0.5	nm	nm
A21	Cu?	67309	0.9	0.7	4.8	25.1	0.5	bdl	bdl	1.7	4.1	bdl	0.4	61.7	bdl	nm	bdl	nm	nm
A22	Fe?	67208	0.8	1.4	6.1	55.1	0.7	bdl	bdl	2.4	12.0	0.6	bdl	21.2	bdl	nm	bdl	nm	nm
A23	Fe?	67398	1.0	1.7	6.9	57.7	1.0	bdl	bdl	3.5	12.0	0.7	bdl	15.9	bdl	nm	bdl	nm	nm

571

572 Table 3. Bulk chemistry of Ashkelon slags analyzed via SEM-EDS, reported as normalized oxide wt.%. Compositions are an average
573 of at least four separate area analyses. Detection limit was empirically determined through examination of raw spectra to be 0.3 wt.%.
574 Empirical examination of EDS spectra 0.25 wt.%. Elements that were quantified but below this threshold are indicated by “bdl.”
575 Elements not measured—primarily because there was no observable peak distinguishable from background noise—are indicated by
576 “nm.”

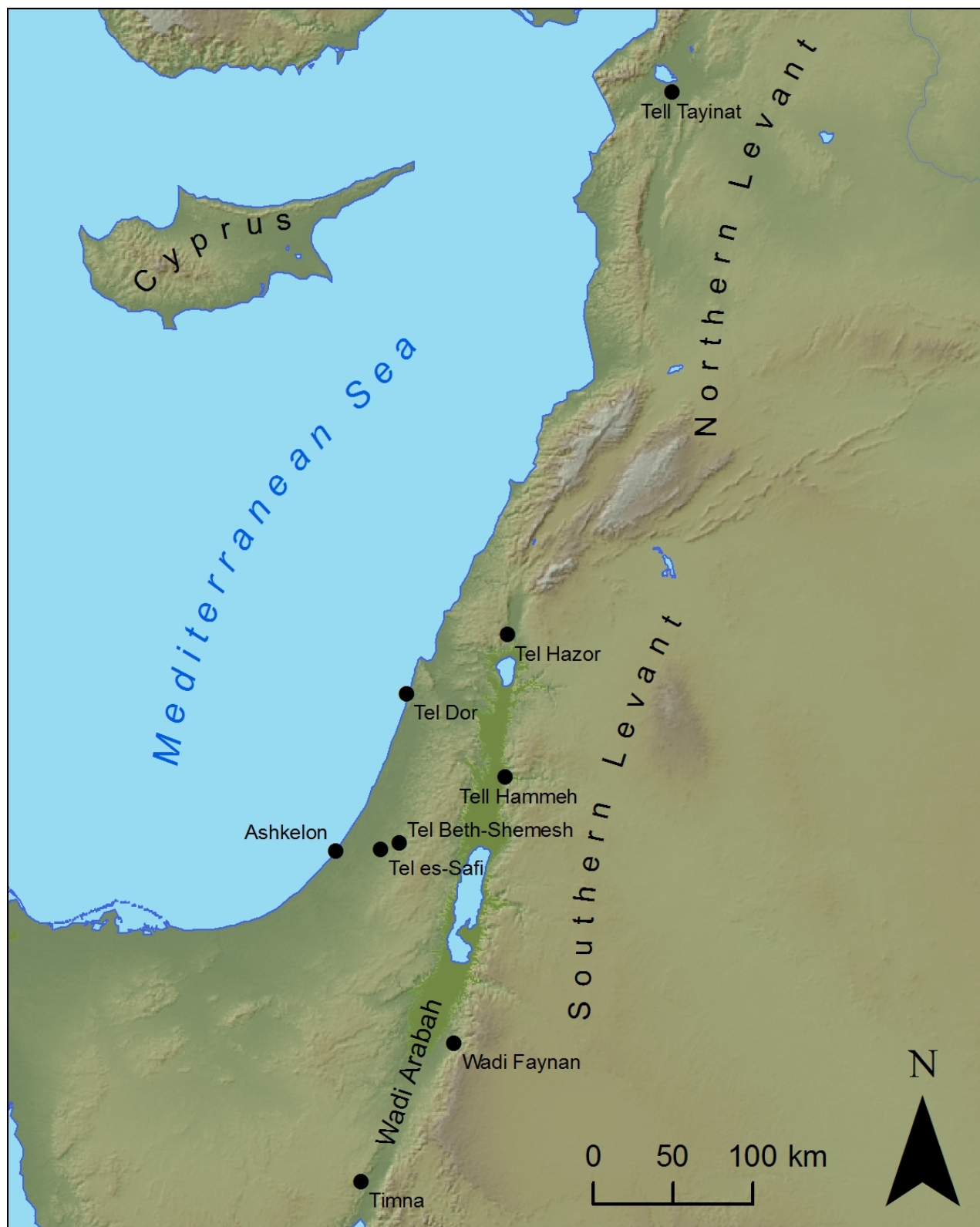
References

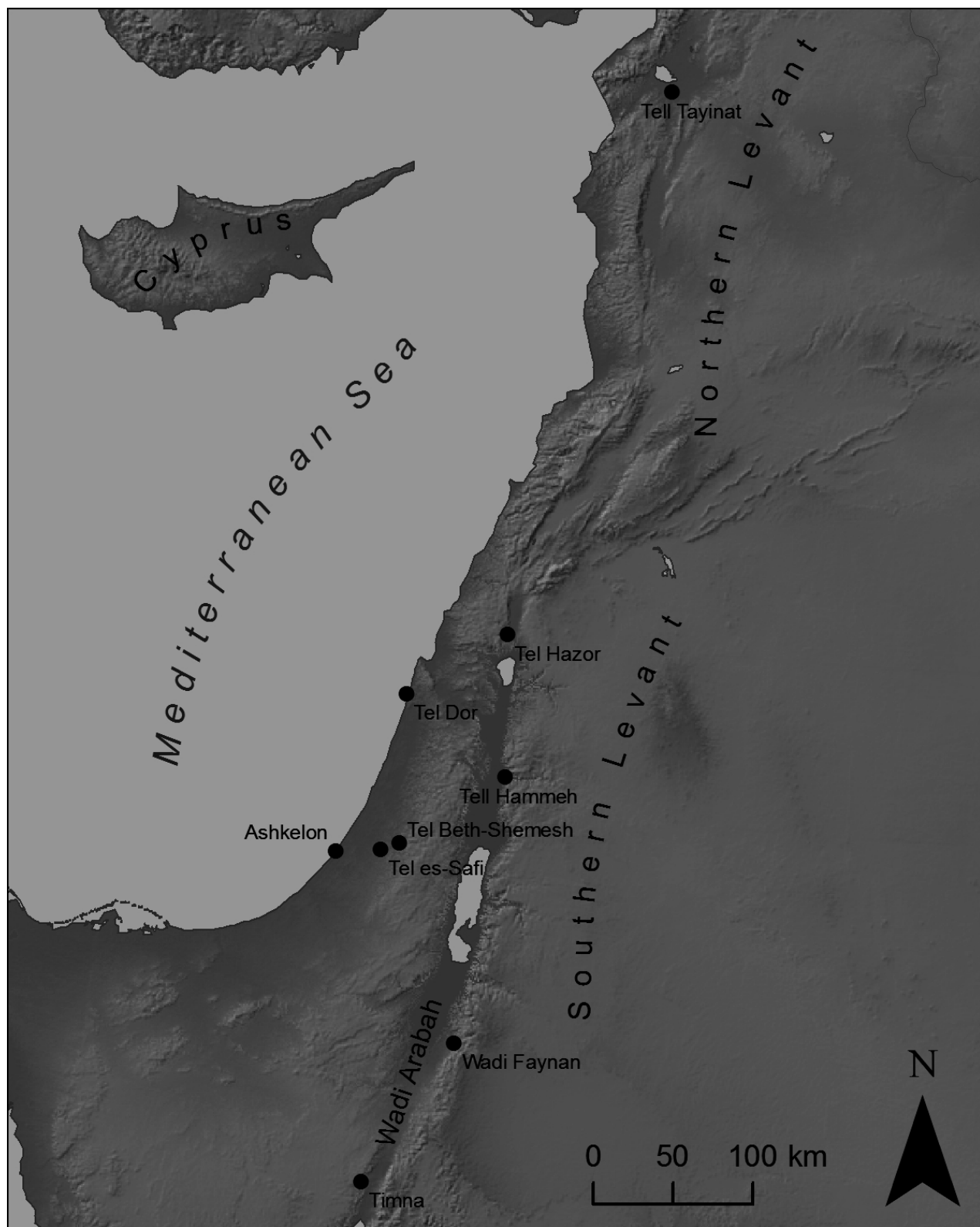
- Aja, A., 2009. Philistine Domestic Architecture, Ph.D Dissertation, Near Eastern Languages and Civilizations, Harvard University, Cambridge, MA.
- Bachmann, H.-G., 1980. Early copper smelting techniques in Sinai and in the Negev as deduced from slag investigations, in: Craddock, P.T. (Ed.), *Scientific Studies in Early Mining and Extractive Metallurgy*, British Museum Occasional Papers, London, pp. 103-134.
- Bachmann, H.-G., 1982. Copper smelting slags from Cyprus: review and classification of analytical data, in: Muhly, J.D., Maddin, R., Karageorghis, V. (Eds.), *Acta of the International Archaeological Symposium on Early Metallurgy in Cyprus, 4,000-500 BC*, Larnaca, Cyprus 1-6 June 1981, Pierides Foundation, Nicosia, pp. 143-151.
- Ben-Yosef, E., Levy, T.E., Higham, T., Najjar, M., Tauxe, L., 2010. The beginning of Iron Age copper production in the southern Levant: New evidence from Khirbat al-Jariya, Faynan, Jordan, *Antiquity* 84, 724-746.
- Ben-Yosef, E., Shaar, R., Tauxe, L., Ron, H., 2012. A new chronological framework for Iron Age copper production at Timna (Israel), *Bulletin of the American Schools of Oriental Research* 367, 31-71.
- Craddock, P.T., Meeks, N.D., 1987. Iron in Ancient Copper, *Archaeometry* 29, 187-204.
- Eliyahu-Behar, A., Shilstein, S., Raban-Gerstel, N., Goren, Y., Gilboa, A., Sharon, I., Weiner, S., 2008. An integrated approach to reconstructing primary activities from pit deposits: iron smithing and other activities at Tel Dor under Neo-Assyrian domination, *Journal of Archaeological Science* 35, 2895-2908.
- Eliyahu-Behar, A., Yahalom-Mack, N., Shilstein, S., Zukerman, A., Shafer-Elliott, Maeir, A.M., Boaretto, E., Finkelstein, I., Weiner, S., 2012. Iron and bronze production in Iron Age IIA Philistia: New evidence from Tell es-Safi/Gath, Israel, *Journal of Archaeological Science* 39, 255-267.
- Eliyahu-Behar, A., Yahalom-Mack, N., Gadot, Y., Finkelstein, I., 2013. Iron smelting and smithing in major urban centers in Israel during the Iron Age, *Journal of Archaeological Science* 40, 4319-4330.
- Erb-Satullo, N.L., Gilmour, B.J.J., Khakhutaishvili, N., 2015. Crucible technologies in the Late Bronze-Early Iron Age South Caucasus: Copper processing, tin bronze production, and the possibility of local tin ores *Journal of Archaeological Science* 61, 260-276.
- Golden, J., Levy, T.E., Hauptmann, A., 2001. Recent discoveries concerning Chalcolithic metallurgy at Shiqmim, Israel, *Journal of Archaeological Science* 28, 951-963.

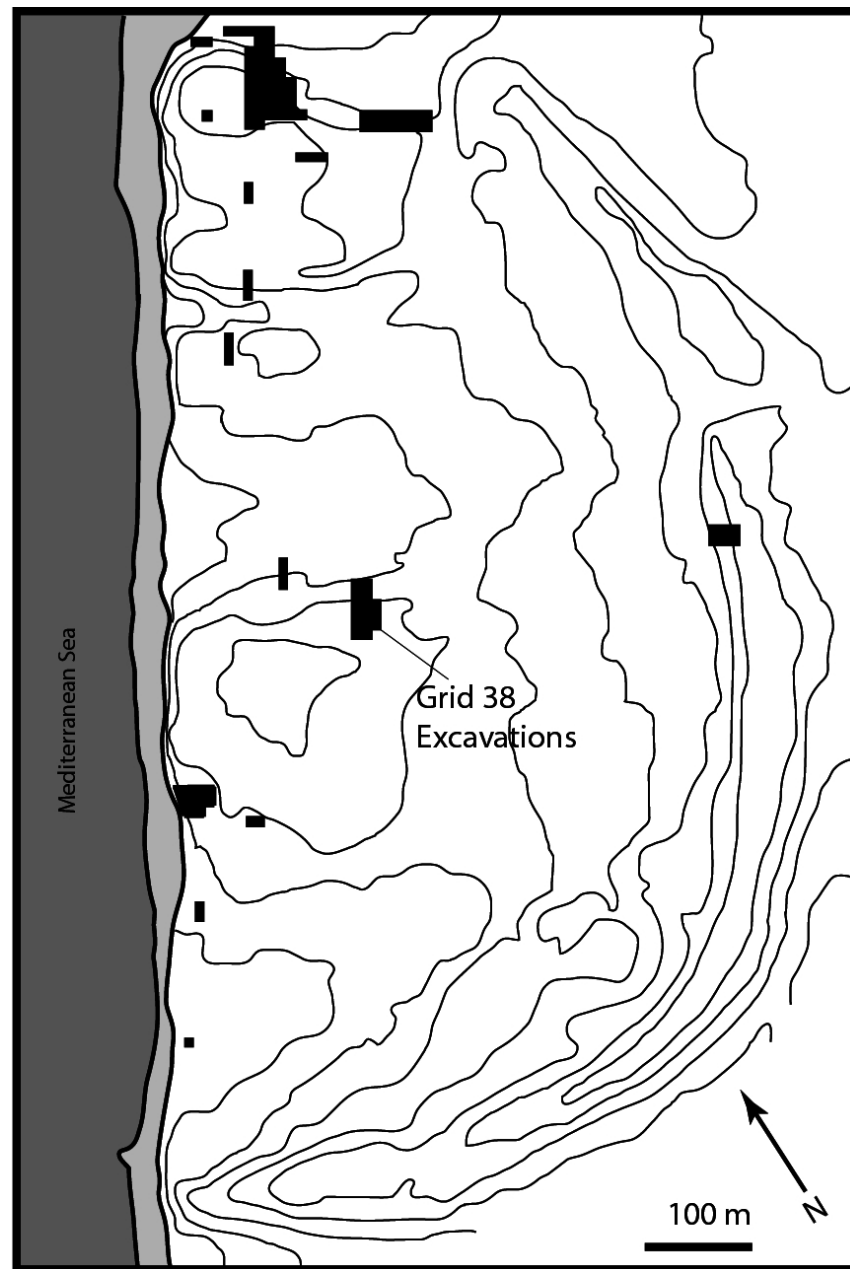
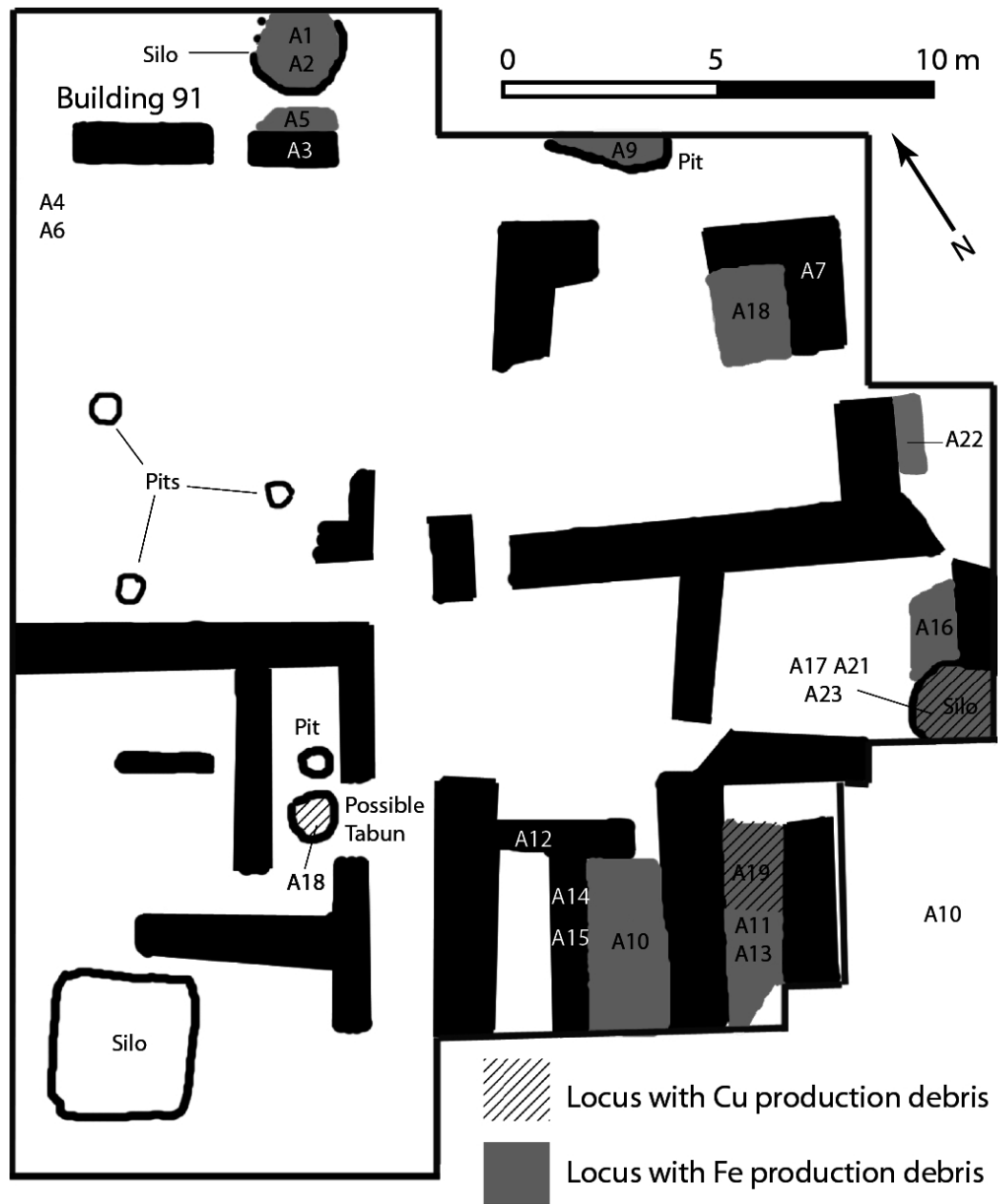
- Gordon, R.B., 1997. Process deduced from ironmaking wastes and artefacts, *Journal of Archaeological Science* 24, 9-18.
- Greenfield, H.J., Miller, D., 2004. Spatial patterning of Early Iron Age metal production at Ndondondwane, South Africa: the question of cultural continuity between the Early and Late Iron Ages, *Journal of Archaeological Science* 31, 1511-1532.
- Hauptmann, A., 2007. The archaeometallurgy of copper: evidence from Faynan, Jordan, Springer, Berlin.
- Killick, D., Miller, D., 2014. Smelting of magnetite and magnetite-ilmenite iron ores in the northern Lowveld, South Africa, ca. 1000 CE to ca. 1880 CE, *Journal of Archaeological Science* 43, 239-255.
- Koucky, F.L., Steinberg, A., 1982. The ancient slags of Cyprus, in: Muhly, J.D., Maddin, R., Karageorghis, V. (Eds.), *Acta of the International Archaeological Symposium on Early Metallurgy in Cyprus, 4,000-500 BC, Larnaca, Cyprus 1-6 June 1981*, Pierides Foundation, Nicosia, pp. 117-137.
- Lechtman, H.N., 1977. Style in technology—Some early thoughts, in: Lechtman, H.N., Merrill, R.S. (Eds.), *Material culture: styles, organization, and dynamics of technology*, West Publishing, pp. 3-20.
- Levy, T.E., Shalev, S., 1989. Prehistoric metalworking in the southern Levant: Archaeometallurgical and social perspectives, *World Archaeology* 20, 352-372.
- Levy, T.E., Adams, R.B., Najjar, M., Hauptmann, A., Anderson, J.D., Brandl, B., Robinson, M.A., Higham, T., 2004. Reassessing the chronology of Biblical Edom: New excavations and ¹⁴C dates from Khirbat en-Nahas (Jordan), *Antiquity* 78, 865-879.
- Levy, T.E., Higham, T., Bronk Ramsey, C., Smith, N.G., Ben-Yosef, E., Robinson, M., Munger, S., Knabb, K., Schulze, J.P., Najjar, M., Tauxe, L., 2008. High-precision radiocarbon dating and historical biblical archaeology in southern Jordan, *Proceedings of the National Academy of Sciences* 105, 16460-16465.
- Maddin, R., Muhly, J.D., Wheeler, T.S., 1977. How the Iron Age began, *Scientific American* 237, 122-131.
- McNutt, P., 1990. *The forging of Israel: iron technology, symbolism and tradition in ancient society*, Almond Press, Decatur, GA.
- Miller, D., Killick, D., 2004. Slag identification at southern African archaeological sites, *Journal of African Archaeology* 2, 23-48.

- Mirau, N.A., 1997. Social context of early ironworking in the Levant, in: Aufrecht, W.A., Mirau, N.A., Gauley, S.W. (Eds.), *Urbanism in Antiquity: From Mesopotamia to Crete*, Sheffield Academic Press, Sheffield, UK, pp. 99-115.
- Muhly, J.D., 1992. The crisis years in the Mediterranean World: transition or cultural disintegration, in: Ward, W.A., Sharp Joukowsky, M. (Eds.), *The Crisis Years: The 12th century BC. From Beyond the Danube to the Tigris*, Kendall/Hunt Publishing, Dubuque, IA, pp. 10-26.
- Rehren, Th., 2012. Iron smithing slag at Reykholt, in: Sveinbjarnardottir, G. (Ed.), *Reykholt: Archaeological Investigations at a high status farm in western Iceland.*, pp. 347-351.
- Rehren, Th., Boscher, L., Pernicka, E., 2012. Large scale smelting of speiss and arsenical copper at Early Bronze Age Arisman, Iran, *Journal of Archaeological Science* 39, 1717-1727.
- Roames, J., 2011. The Early Iron Age metal workshop at Tell Tayinat, Turkey, in: Vandiver, P., Li, W., Ruvalcaba Sil, J.L., Reedy, C.L., Frame, L.D. (Eds.), *Materials Issues in Art and Archaeology IX*, Cambridge University Press, Cambridge, pp. 149-155.
- Shugar, A., 2003. Reconstructing the chalcolithic metallurgical process at Abu Matar, Israel, *International Conference: Archaeometallurgy in Europe*, Associazione italiana di metallurgia, Milan, Italy, pp. 449-458.
- Snodgrass, A.M., 1971. *The dark age of Greece: an archaeological survey of the eleventh to the eighth centuries BC*, Edinburgh University Press, Edinburgh.
- Snodgrass, A.M., 1980. Iron and early metallurgy in the Mediterranean, in: Wertime, T.A., Muhly, J.D. (Eds.), *The Coming of the Age of Iron*, Yale University Press, New Haven, pp. 335-374.
- Soullignac, R., 2017. *Les Scories de Forge du Pays Dogon (Mali): Entre Ethnoarchéologie, Archéologie Expérimentale et Archéométrie*, LIBRUM, Hochwald/Basel, Switzerland.
- Stager, L.E., Master, D.M., Schloen, J.D., 2011. *Ashkelon 3: The Seventh Century BC*, Eisenbrauns, Winona Lake, IN.
- Thornton, C.P., Rehren, Th., Pigott, V.C., 2009. The production of speiss (iron arsenide) during the Early Bronze Age in Iran, *Journal of Archaeological Science* 36, 308-316.
- Tylecote, R.F., Ghaznavi, H.A., Boydell, P.J., 1977. Partitioning of trace elements between ores, fluxes, slags and metal during the smelting of copper, *Journal of Archaeological Science* 4, 305-333.
- Van Beek, G.W., Van Beek, O., 2008. *Glorious Mud! Ancient and Contemporary Earthen Design and Construction in North Africa, Western Europe, the Near East, and Southwest Asia*, Smithsonian Institution Scholarly Press, Washington, DC.

- Veldhuijzen, H.A., 2005. Early Iron Production in the Levant: Smelting and Smithing at Early 1st Millennium BC Tell Hammeh, Jordan, and Tel Beth Shemesh, Israel, PhD Thesis, Institute of Archaeology, University College London, London.
- Veldhuijzen, H.A., Rehren, Th., 2007. Slags and the city: Early iron production at Tell Hammeh, Jordan and Tel Beth-Shemesh, Israel, in: La Niece, S., Hook, D., Craddock, P. (Eds.), *Metals and Mines: Studies in Archaeometallurgy*, Archetype Publications, London, pp. 189-201.
- Veldhuijzen, H.A., 2009. Red hot: the smithy at Tel Beth-Shemesh, *Near Eastern Archaeology* 72, 129-131.
- Veldhuijzen, H.A., 2012. Just a few rusty bits: The innovation of iron in the Eastern Mediterranean in the 2nd and 1st millennia BC, in: Kassianidou, V., Papasavvas, G. (Eds.), *Eastern Mediterranean Metallurgy and Metalwork in the Second Millennium BC*, Oxbow Books, Oxford, pp. 237-250.
- Yahalom-Mack, N., Gadot, Y., Eliyahu-Behar, A., Bechar, S., Shilstein, S., Finkelstein, I., 2014a. Metalworking at Hazor: A long-term perspective, *Oxford Journal of Archaeology* 33, 19-45.
- Yahalom-Mack, N., Galili, E., Segal, I., Eliyahu-Behar, A., Boaretto, E., Shilstein, S., Finkelstein, I., 2014b. New insights into Levantine copper trade: analysis of ingots from the Bronze and Iron Ages in Israel, *Journal of Archaeological Science* 45, 159-177.
- Yahalom-Mack, N., Eliyahu-Behar, A., 2015. The transition from bronze to iron in Canaan: Chronology, technology and context, *Radiocarbon* 57, 285-205.







Slag Cakes from Iron Production

A3 - Top View



A5 - Section



A15 - Section



5 cm



Silica-rich Slag

A22



2 cm

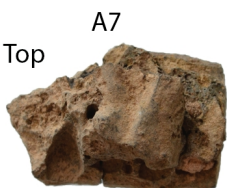


Tap Slags from Iron Production

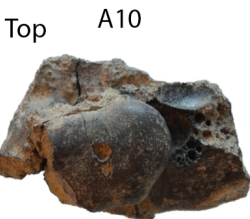
A1



5 cm



Bottom

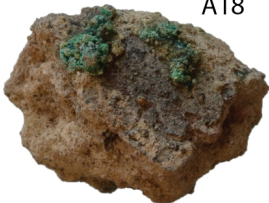


Bottom



Copper Production Slags

A18



A19



2 cm

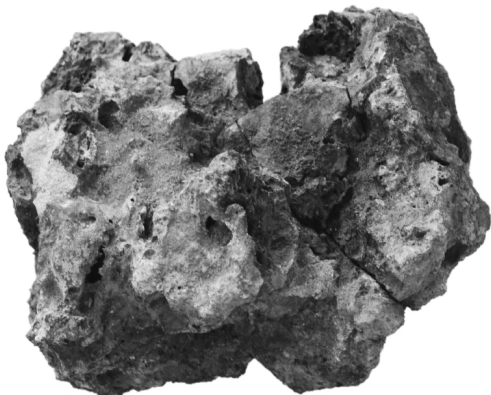


A20

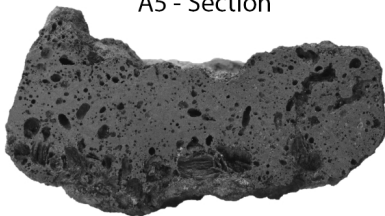


Slag Cakes from Iron Production

A3 - Top View



A5 - Section



A15 - Section



5 cm



Silica-rich Slag

A22



2 cm

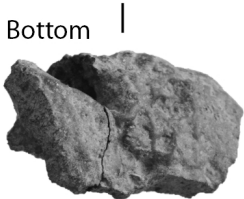
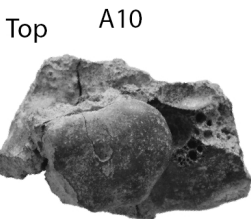
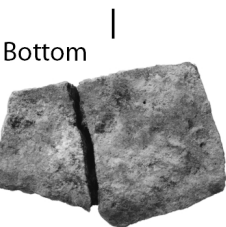
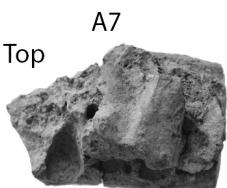


Tap Slags from Iron Production

A1



5 cm



Copper Production Slags

A18



A19



A20

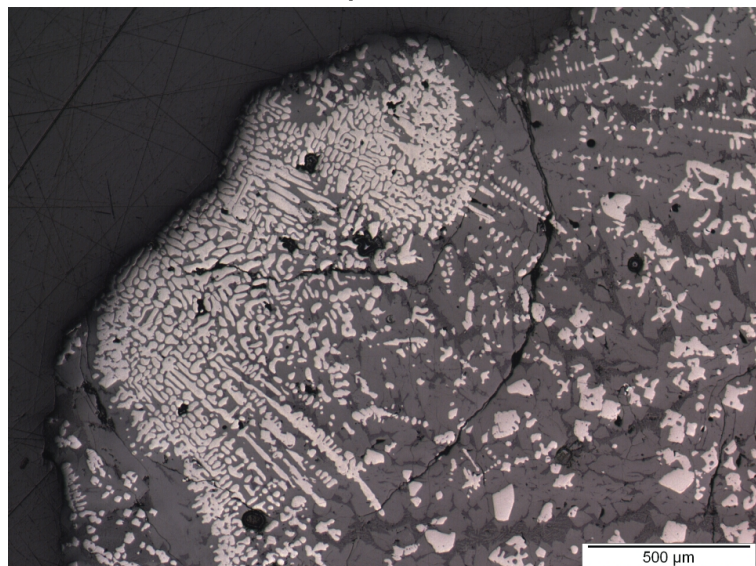


2 cm



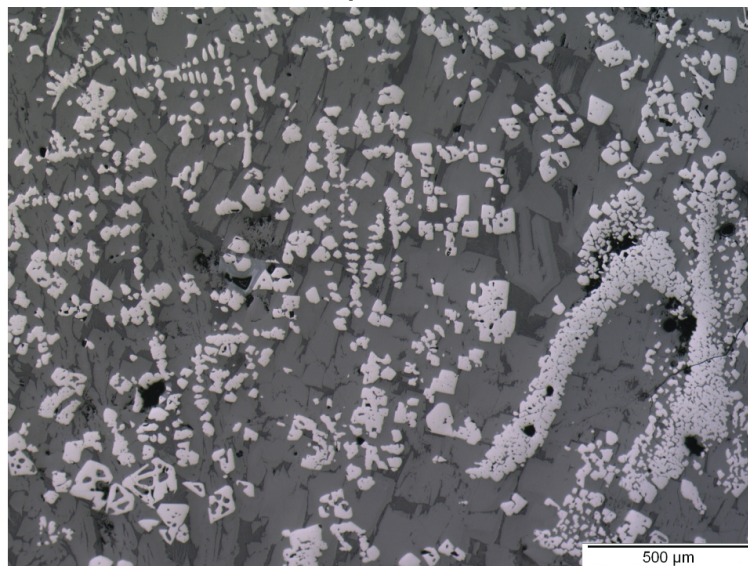
A

Sample A4



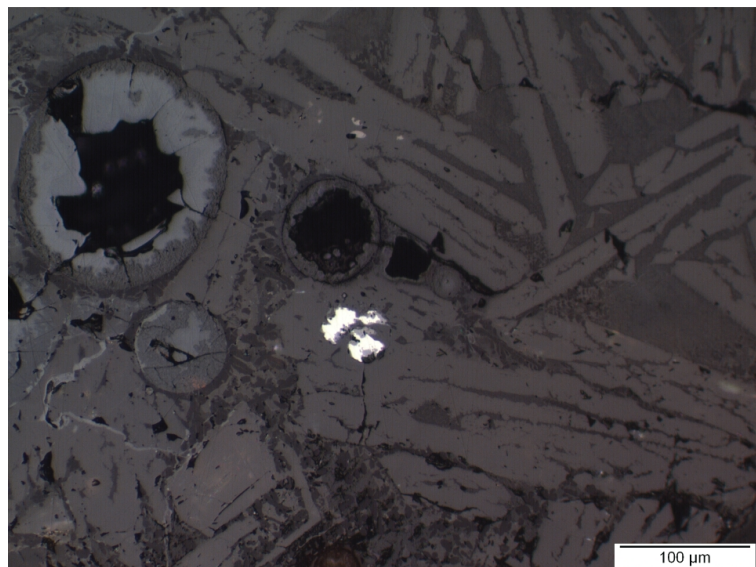
B

Sample A4



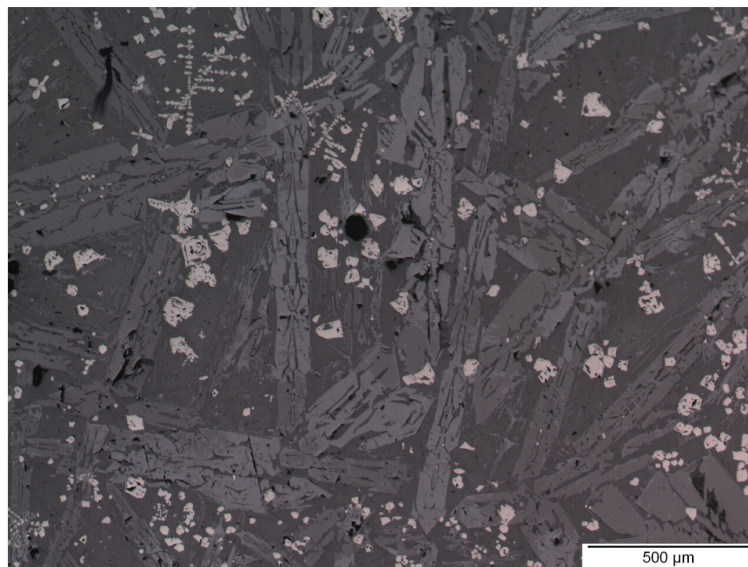
C

Sample A15



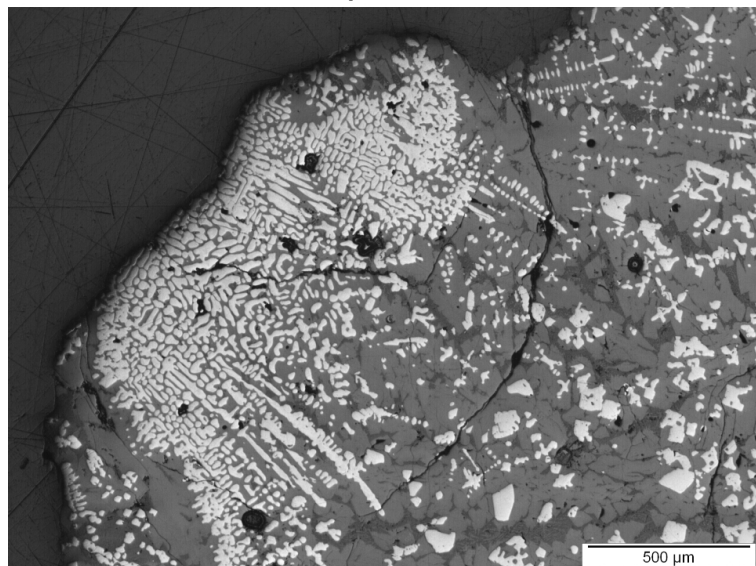
D

Sample A15



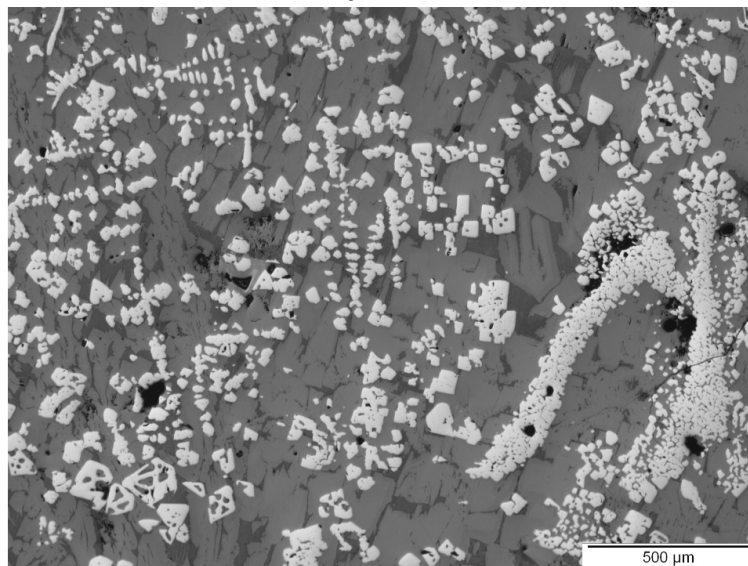
A

Sample A4



B

Sample A4



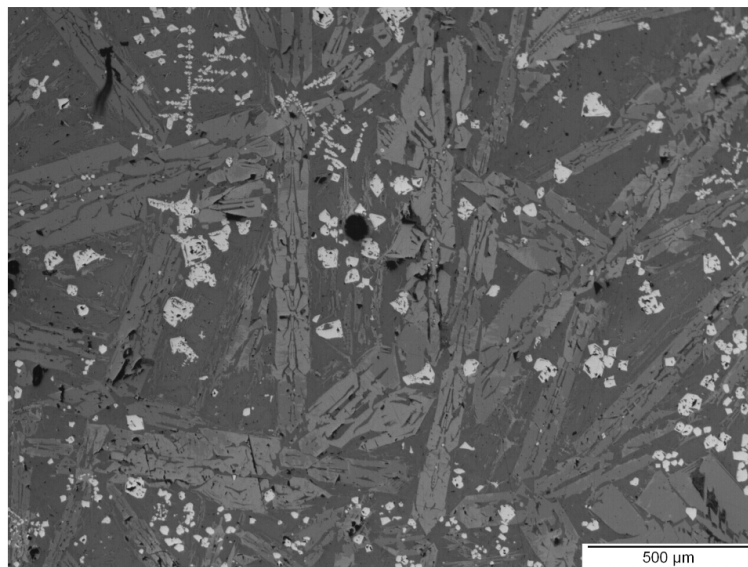
C

Sample A15



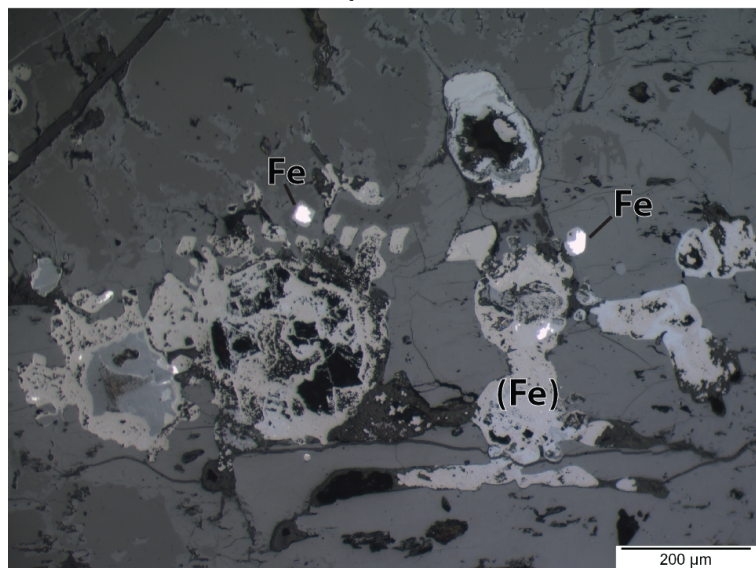
D

Sample A15



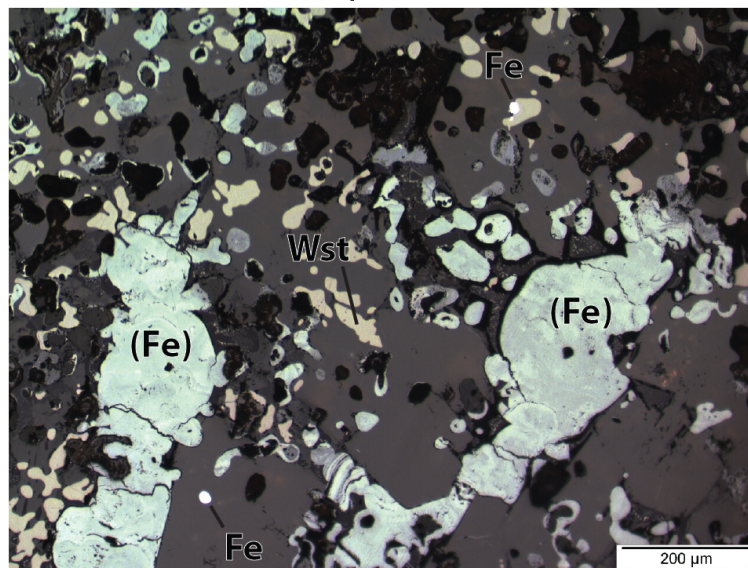
A

Sample A17



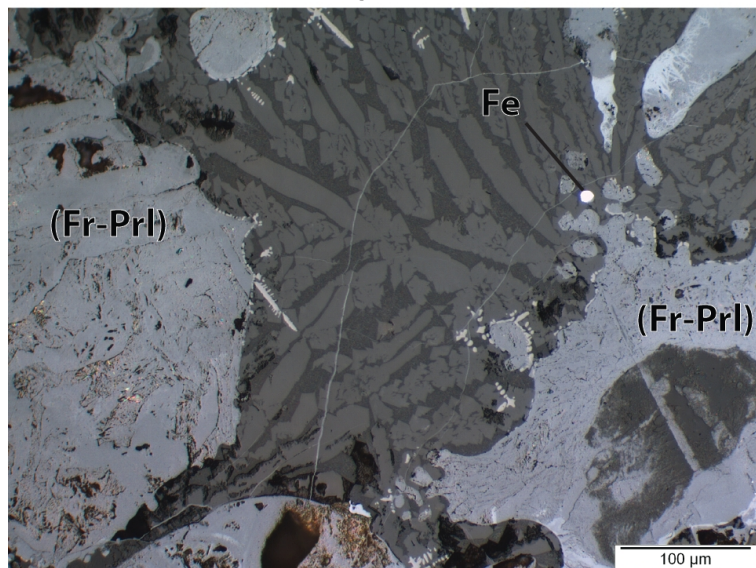
B

Sample A5



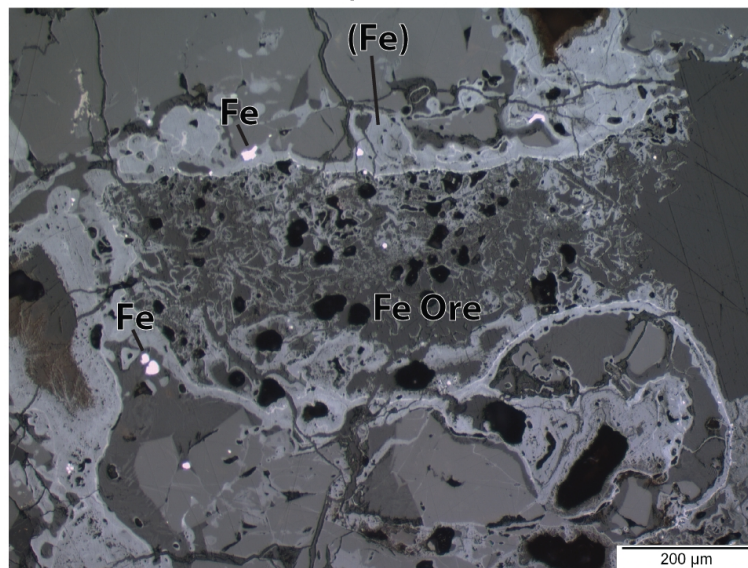
C

Sample A8



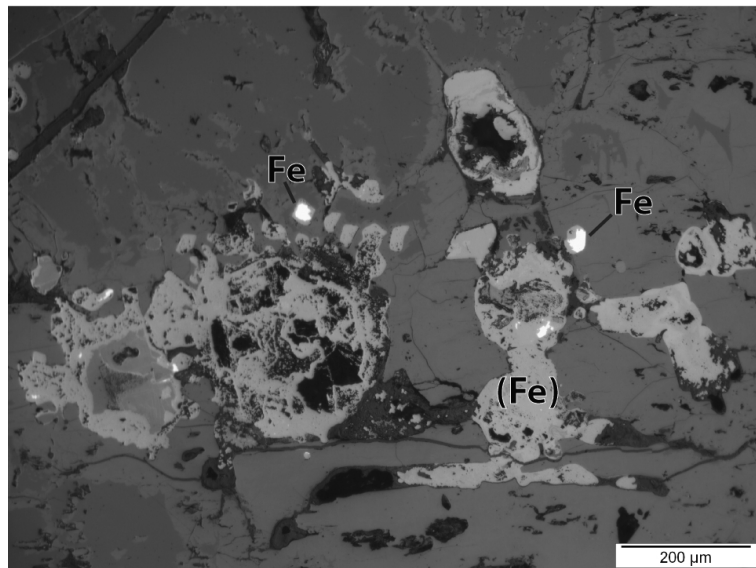
D

Sample A17



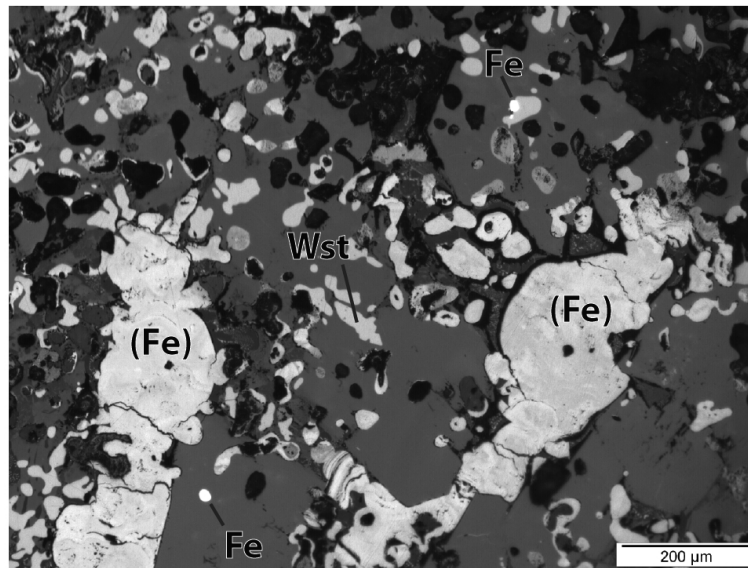
A

Sample A17



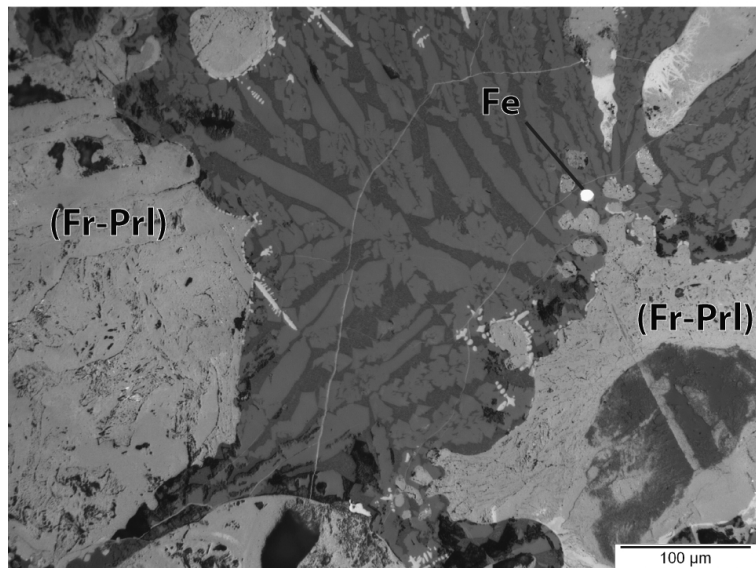
B

Sample A5



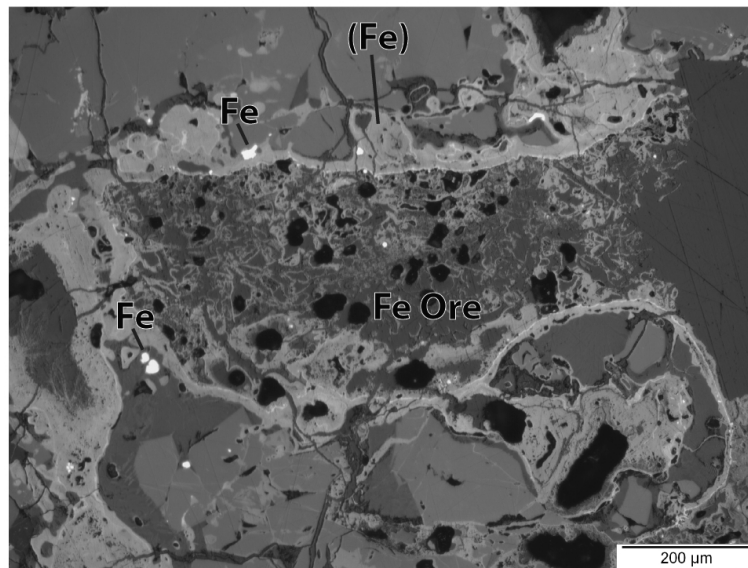
C

Sample A8



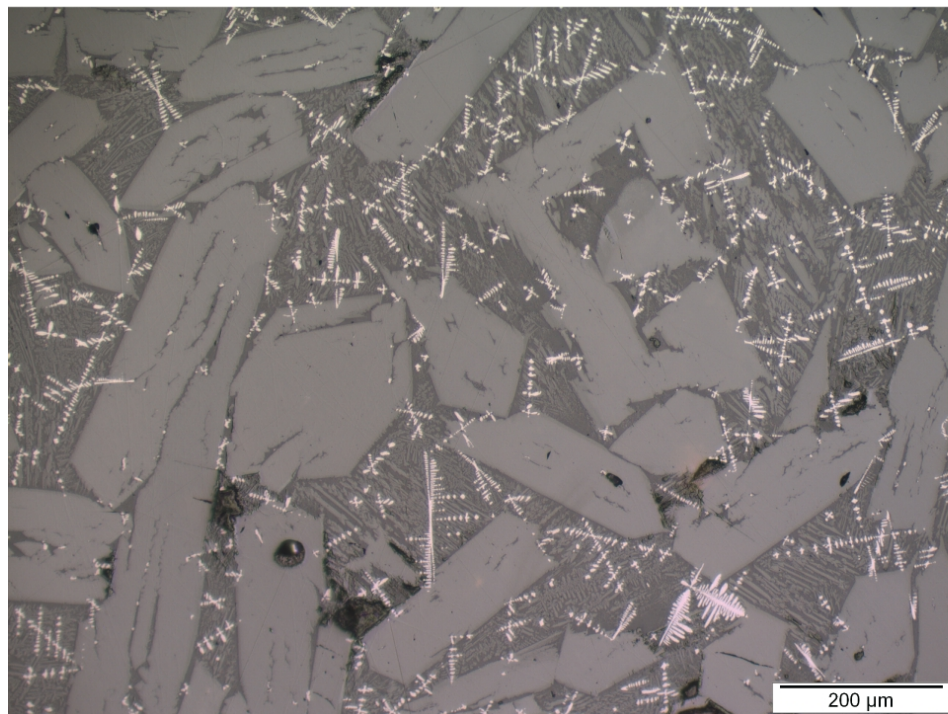
D

Sample A17



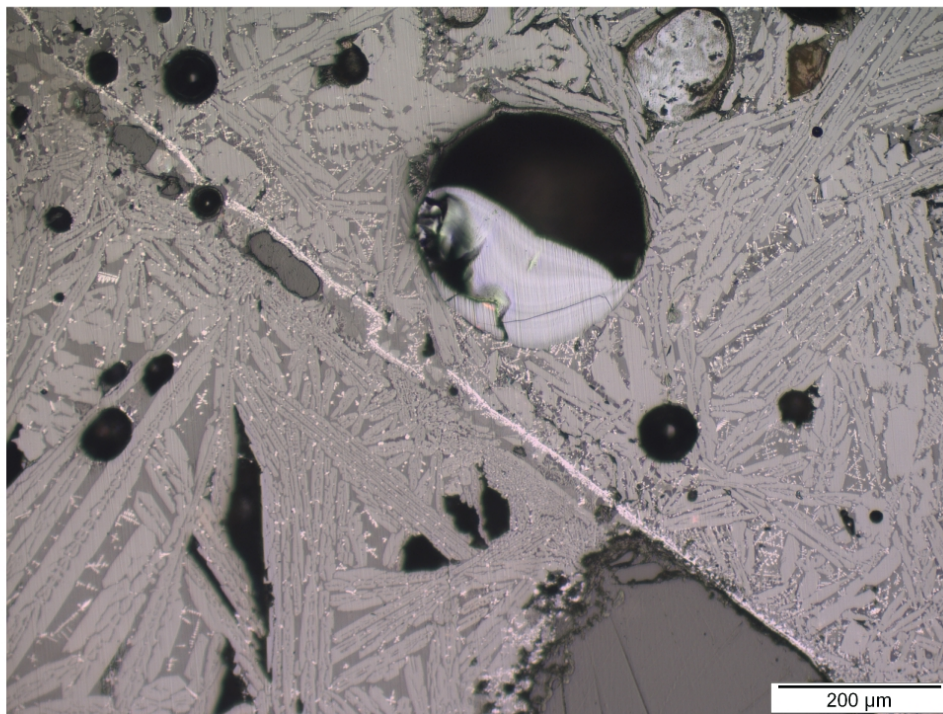
A

Sample A10



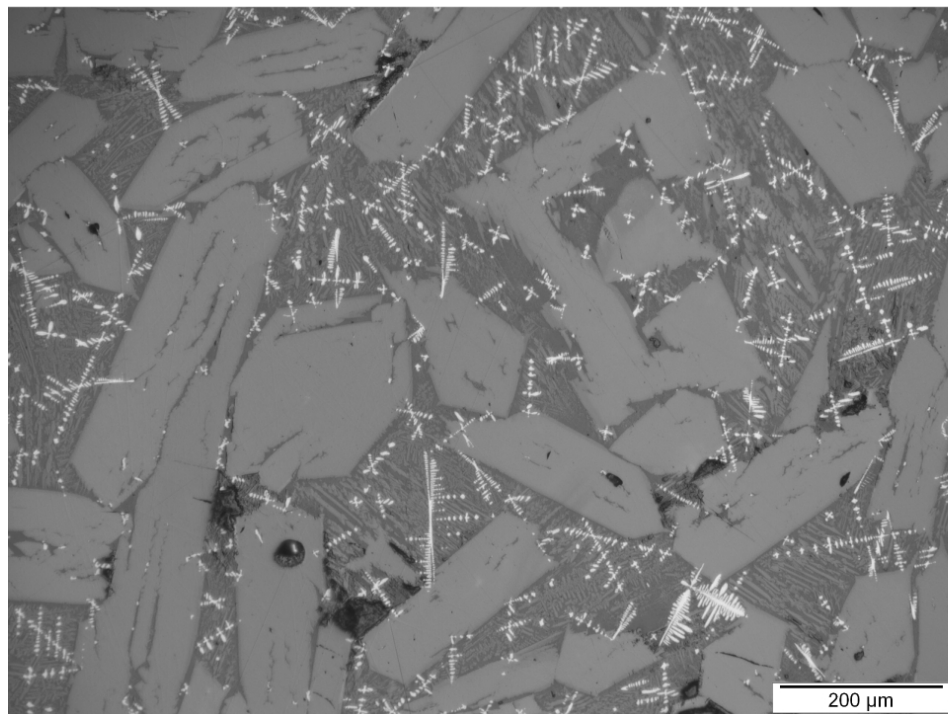
B

Sample A7



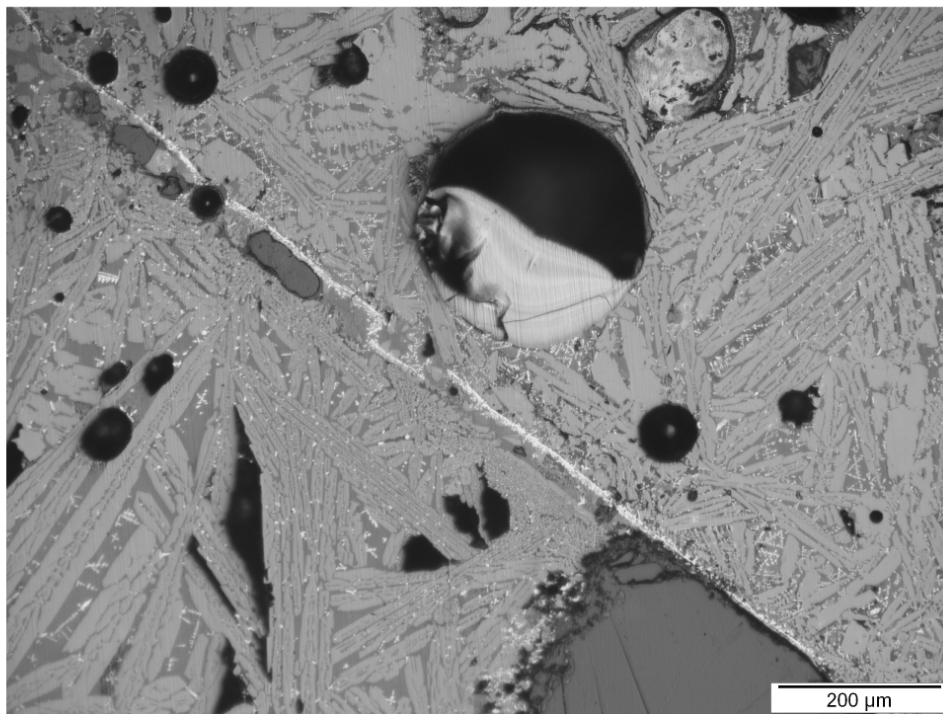
A

Sample A10



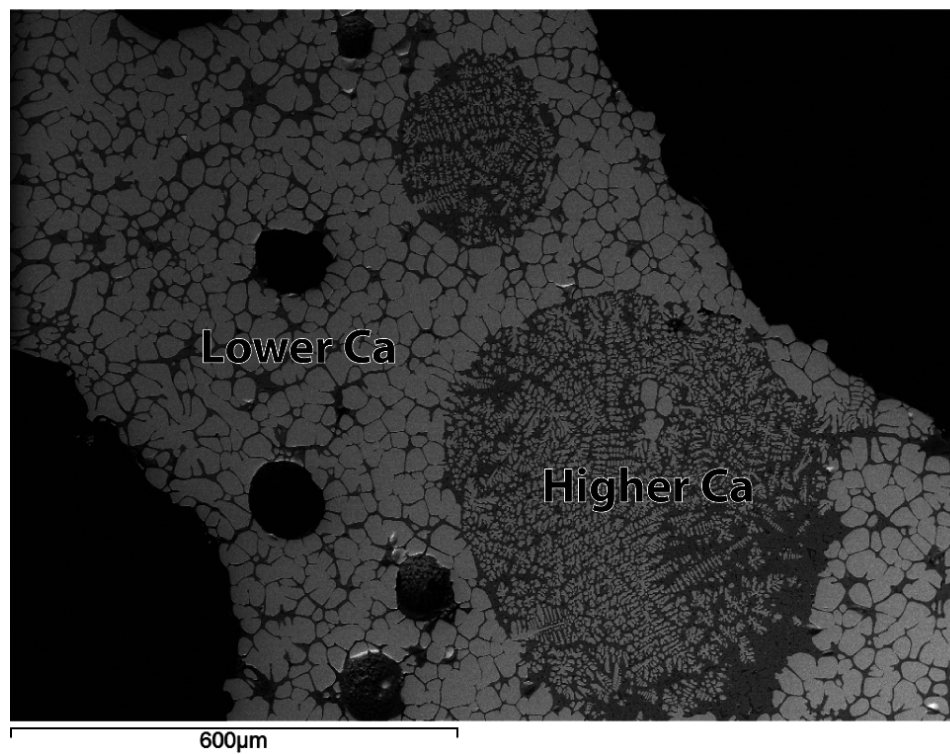
B

Sample A7



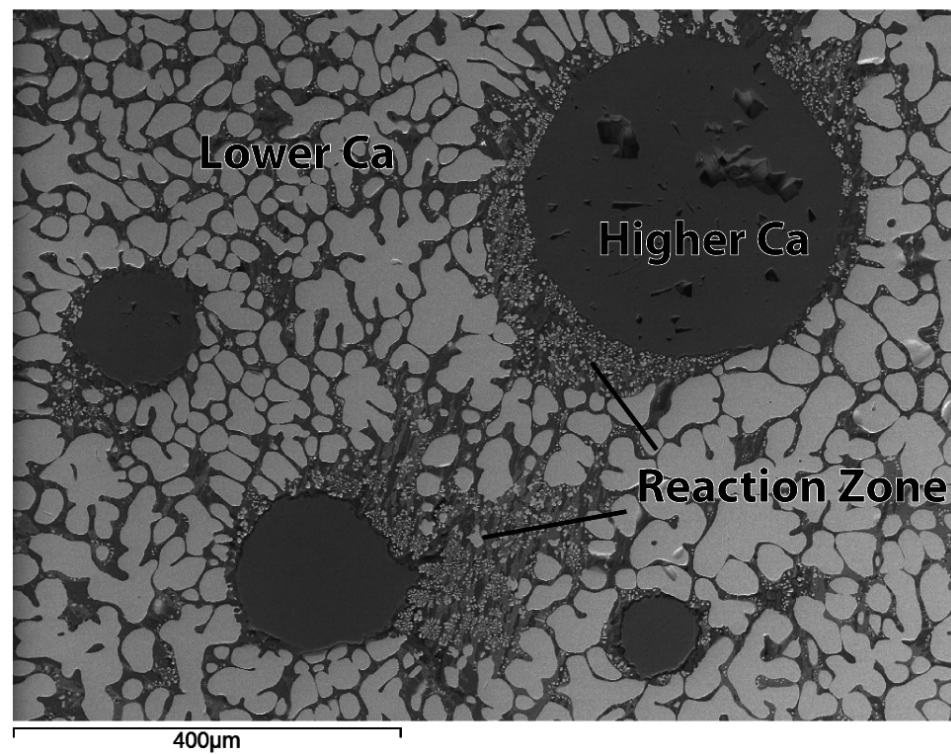
A

Sample A1



B

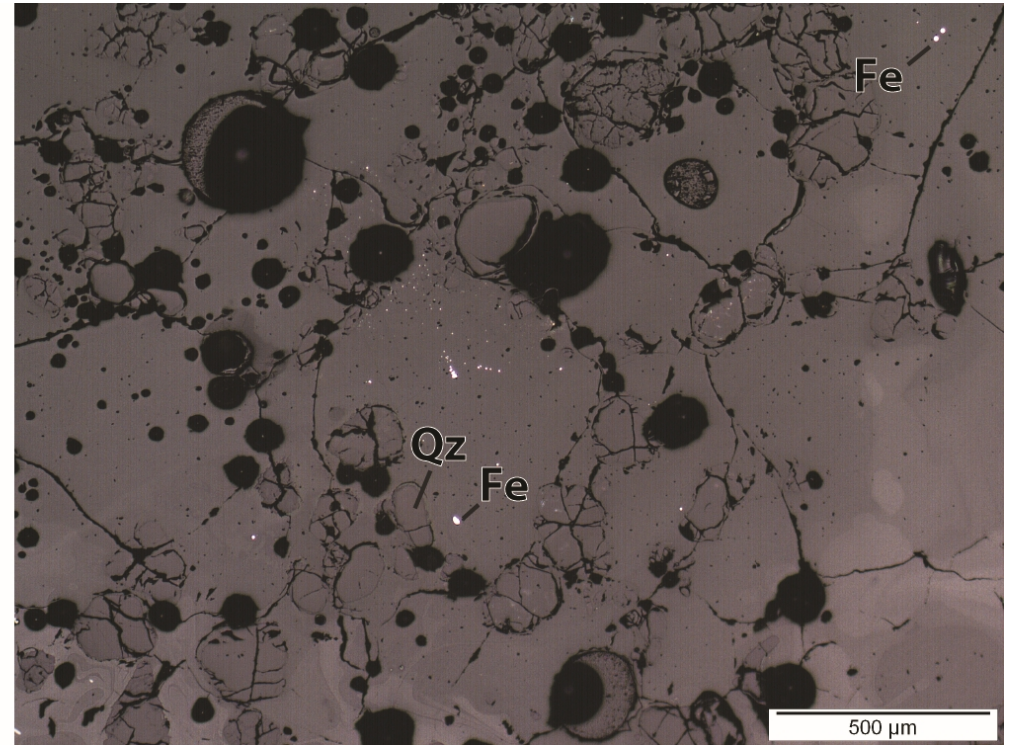
Sample A2



Sample A14



5 cm

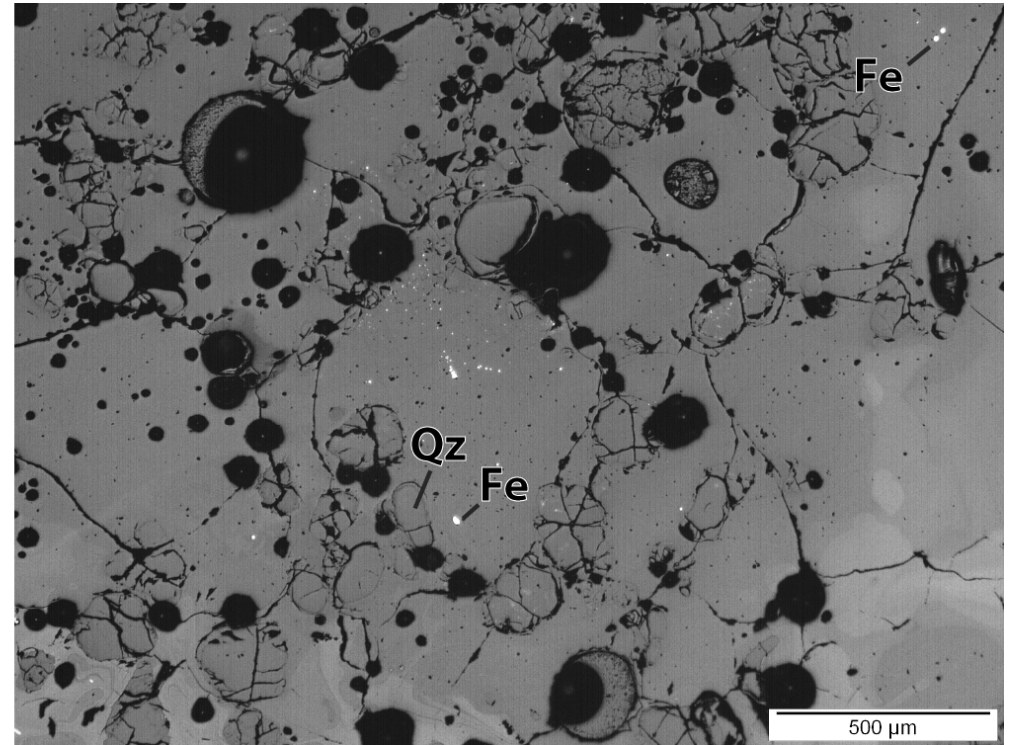


500 μm

Sample A14



5 cm



Fe

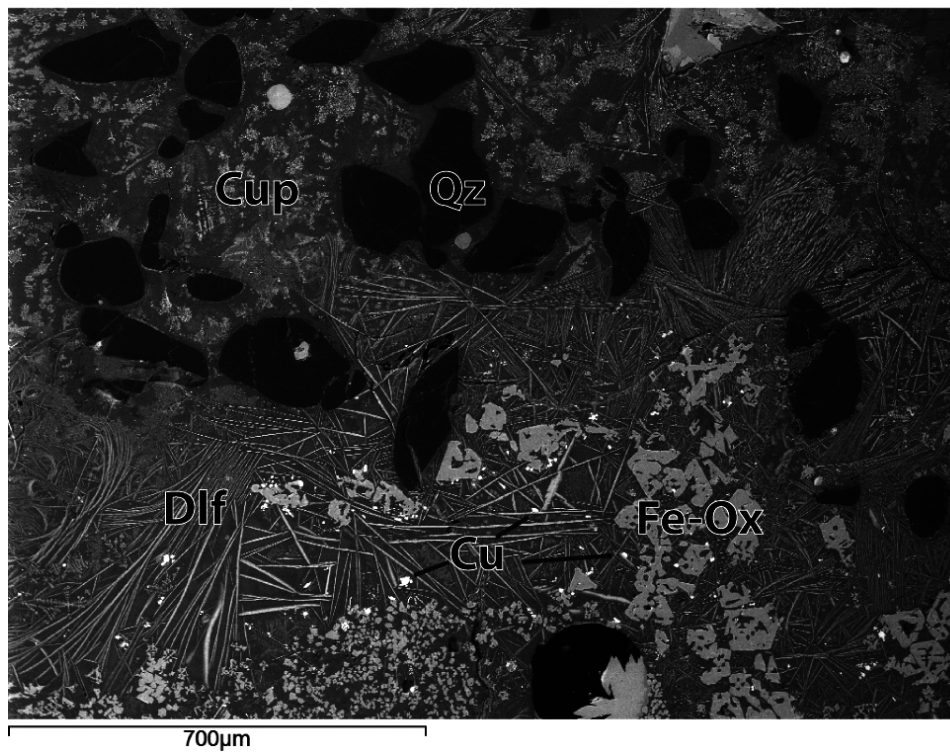
Qz

Fe

500 μm

A

Sample A19



B

Sample A20

